

Supplementary materials

Supplementary material includes following files:

1. Additional methods and results
2. Supplementary figures S1–S40
3. Supplementary tables S1–S19
4. Dataset used in phylogenetic analysis
5. Supplementary data S1–S21 (separated Excel File)

Additional methods and results:

Tip-dated Bayesian analyses. We also performed Bayesian analyses using Tip-dated methods as in [1], which co-estimates the topology and branch lengths. We first constrained four major clades, the Aves, Ornithothoraces, Enantiornithines and Ornithuromorpha. The Mkv substitution model [2] with gamma rate variation [3] was used for the morphological characters. The fossilized birth-death process was used as the tree prior [4]. The fossil ages were assigned uniform distributions with lower and upper bounds from the corresponding stratigraphic ranges. The root age was assigned an offset exponential prior with mean 170 Ma (slightly older than the first appearance datum of the outgroup Dromaeosauridae) and minimum 153 Ma (slightly older than the first appearance datum of *Archaeopteryx*). The most recent common ancestor of *Anas* and *Gallus* was calibrated using a normal distribution with mean 55 Ma and standard deviation 5 Ma to avoid underestimating its divergence time due to lack of fossils in the crown group [1]. The independent lognormal relaxed clock model was used for the morphological rates [5]. The mean clock rate was assigned a gamma (2, 100) distribution with mean 0.02 (expecting two changes per 100 characters per million years) and the variance of the clock rate was assigned a diffuse exponential prior with mean 2.0. We executed two independent runs with four chains per run for 50 million generations and sampled every 2000 generations. The first 25% of samples were discarded as burn-in for each run, and the remaining samples from the two runs were combined after checking consistency between runs. This tree still has several polytomies within the Enantiornithines and Ornithuromorpha, and these polytomies

were further resolved by constraining to the 50% majority-rule consensus tree of the most parsimonious trees obtained in previous analyses. The Bayesian majority-rule consensus tree is completely resolved (figure S1), and this was used in subsequent analyses. These analyses were conducted in MrBayes (v. 3.2.8) [6].

Analyses of effect of body mass on discrete character morphospace. In order to explore the effects of body mass on the discrete character morphospace (dsMoSp), a rarely discussed issue raised by [7], correlation tests were performed following the pipeline therein. In addition to the taxa included in the dataset of the appendicular limb element length (data 1), body mass of additional 17 taxa that were included in the discrete character matrix were estimated using the same method mentioned in the main text. Collectively, there are 71 Mesozoic birds included in the correlation test between body mass and discrete character morphospace. The phylogenetic backbone is derived from the timed-scaled phylogeny using the “mbl” method. Taxa were pruned from the phylogeny if they lack estimated body mass. The Dromaeosauridae assigned as the outgroup in the phylogenetic analysis has to be excluded in the following analysis, because it represents a “composite” outgroup rather than a specific taxon. *Archaeopteryx* was assigned as the outgroup. The analyses were performed using the R scripts provided in Brougham and Campione (2020), and interested readers shall refer to the original study.

The absolute values of the phylogenetically corrected Pearson correlation between mass and pcoa 1 is 0.43 (table S10). Both the robust linear regression and the pGLS models recovered statistically significant correlation between body mass and pcoa 1,

with the former accounts for 31% and 25% of the variation of the latter. Pcoa 1 is the axis most strongly related to body mass under the pGLS model, and it is the only axis with a correlation coefficient surpassing the two-tailed 95% confidence interval (figure S17b). The values of the remaining pcoas are substantially smaller. Mantel and pGLS tests showed significant correlation between discrete character MORD and body mass Euclidean distance. However, body mass only describes 8.4% and 2.5% of the variation of the discrete character distance matrix (table S10). The observed correlation coefficient falls outside a distribution of randomly generated correlation coefficients via permutations of the distance matrices (figure S17c).

Exhaustion of character space analysis. In order to compare the mode and pattern of morphological disparity between enantiornithines and ornithuromorphs, we performed the exhaustion of character space analysis. The method was outlined in [8], and refer the interested readers there for a more detailed description. The analysis was conducted using the `exhaustionFunctions` of the R paleotree package [9]. We chose the “charAlt” option to plot the total number of character alterations and therefore model the size and distribution of character space. Because discrete characters that were coded as “uncertain” cannot be appropriately imported into the current version of `exhaustionFunctions`, those characters were treated as missing values.

Supplementary Figures

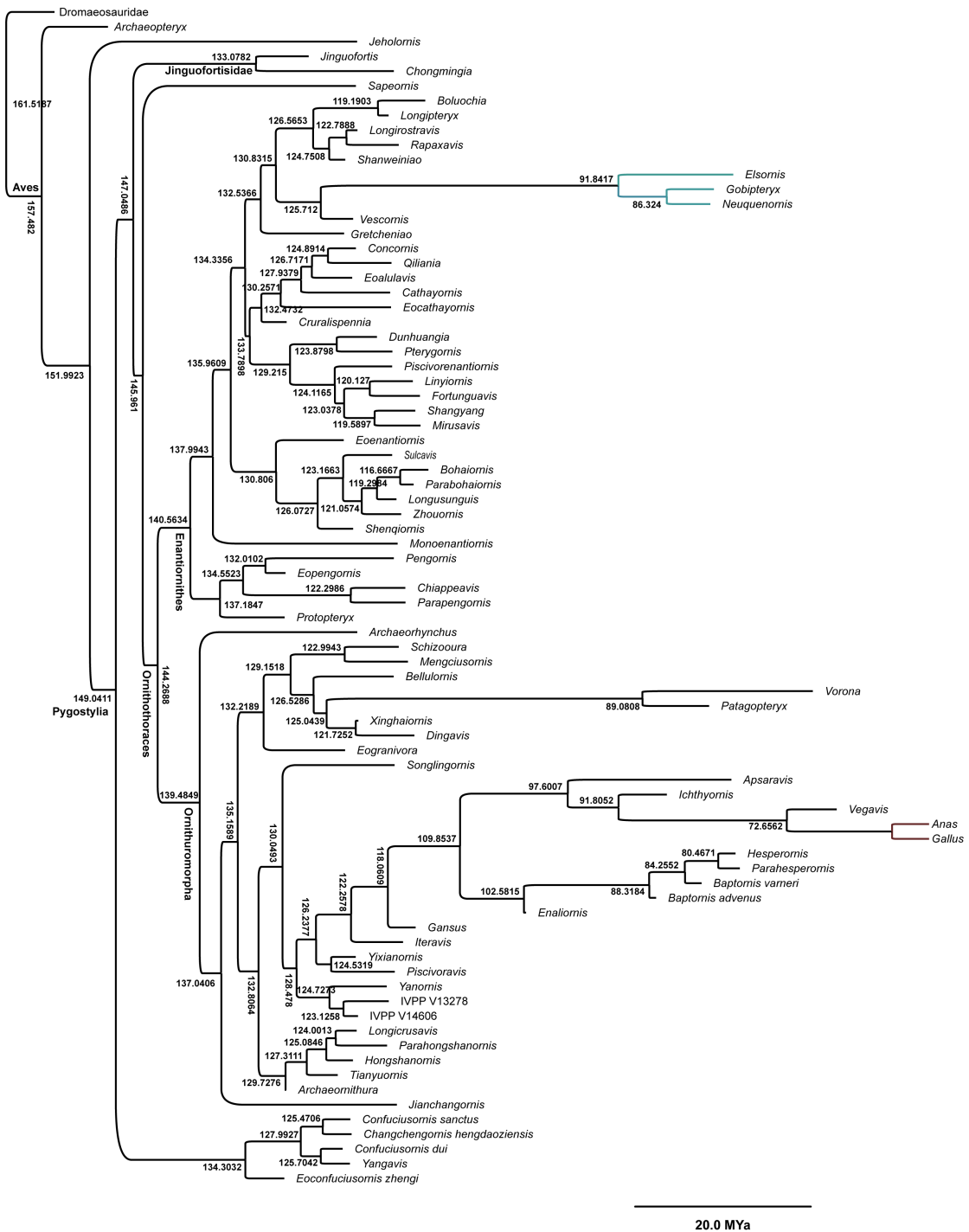


Figure S1. Time-calibrated phylogeny of Mesozoic birds using the tip-dating method.

The tree is derived from the 50% majority rule consensus tree. The median value for each estimated divergence date is shown.

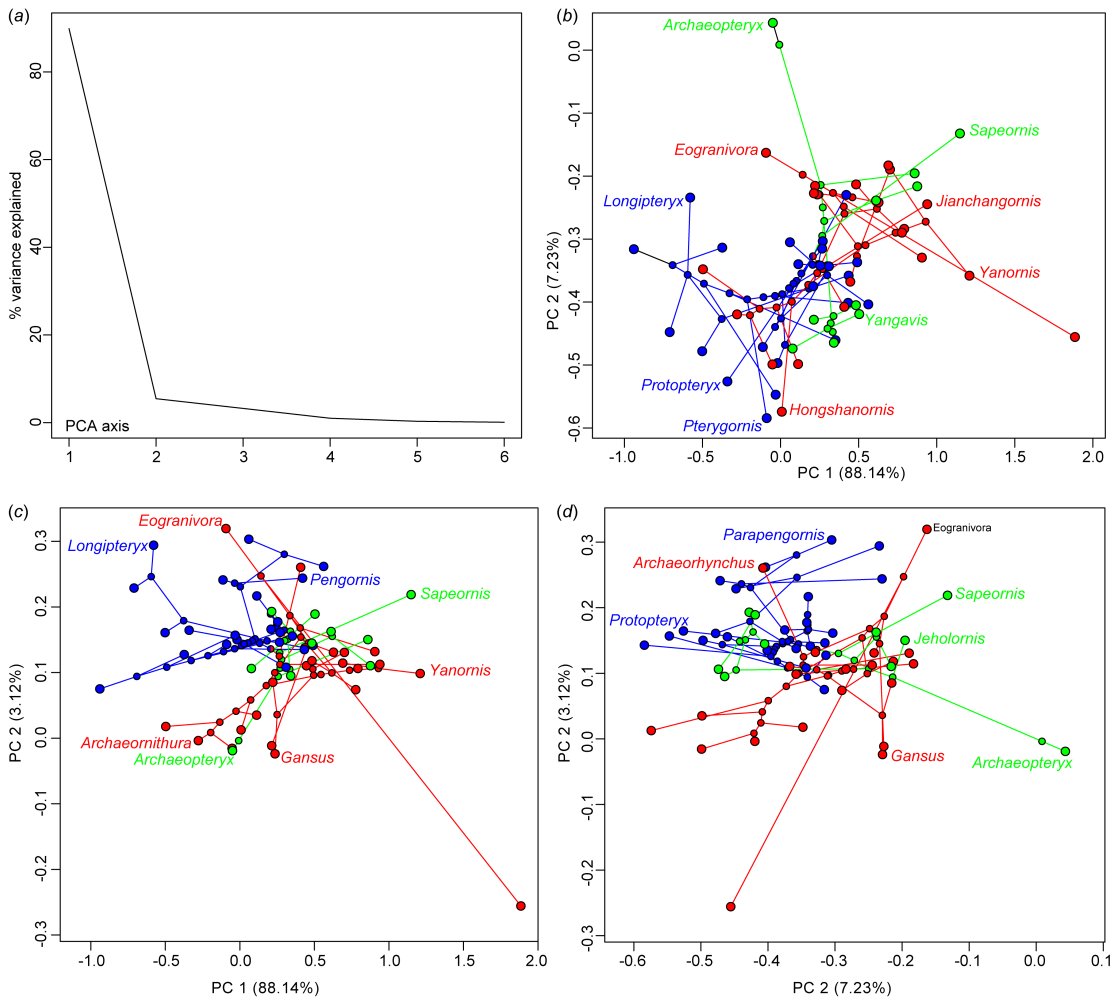


Figure S2. Limb proportions phylomorphospace of Mesozoic birds. The phylogenetic backbone is derived from the “mbl”-scaled strict consensus tree, and the ancestral states were estimated using the lambda method. (a) Proportions of variances accounted by each principal components (PCs) recovered from phylogenetic principal components analysis; (b-d) pairwise binary plots of PCs 1–3. The color scheme repeats that of figure 2.

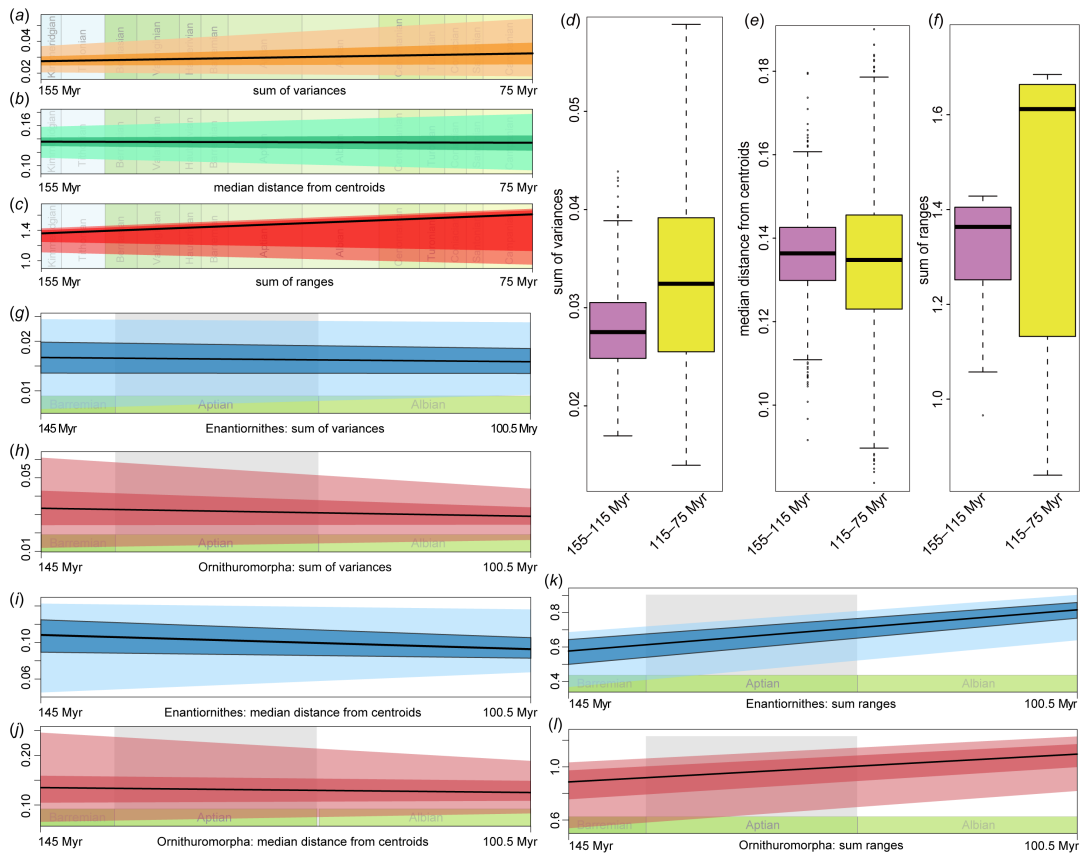


Figure S3. Limb proportions disparity of Mesozoic birds. The phylogenetic backbone is derived from the “mbl”-scaled strict consensus tree. Three disparity metrics are shown: sum of variances, median distance from centroids, and sum of ranges. (a–c) Disparity line of Mesozoic birds across two equal-length time bins (155–115, 115–75 Myr) based on the “mbl”-scaled phylogeny; (d–f) disparity metrics of all taxa as a whole across two equal-length time bins (155–115, 115–75 Myr); (d) box plot showing disparity metrics among Mesozoic avian groups; (g–l) comparison of disparity between Enantiornithes and Ornithuromorpha during the Early Cretaceous in two equal-length time bins (145–125, 125–100.5 Myr). The dark and light shadows indicate the 50% and 95% confidence intervals derived from bootstrap analyses, respectively. For results using the “equal”-scaled and tip-dated phylogenies see the figures S6 and S7.

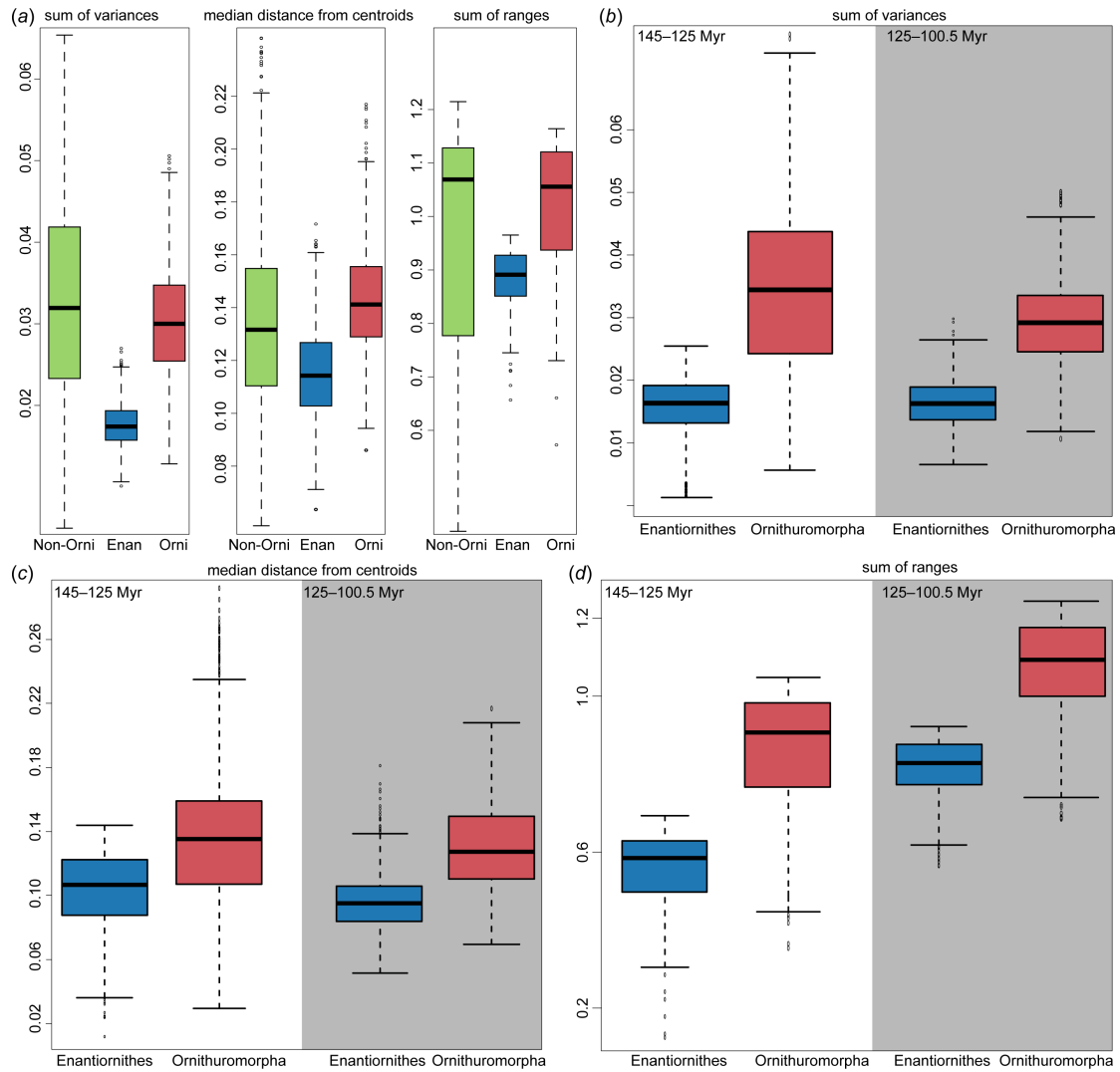


Figure S4. Box plots showing limb proportion disparity of Mesozoic birds with the Late Cretaceous ornithuromorph *Patagopteryx* excluded. The phylogenetic backbone is the “mbl”-scaled phylogeny, and MORD was used as the distance metrics. **(a)** All Mesozoic birds; **(b–d)** comparisons of disparity metrics between Early Cretaceous Enantiornithes and Ornithuromorpha across two subequal-length time bins.

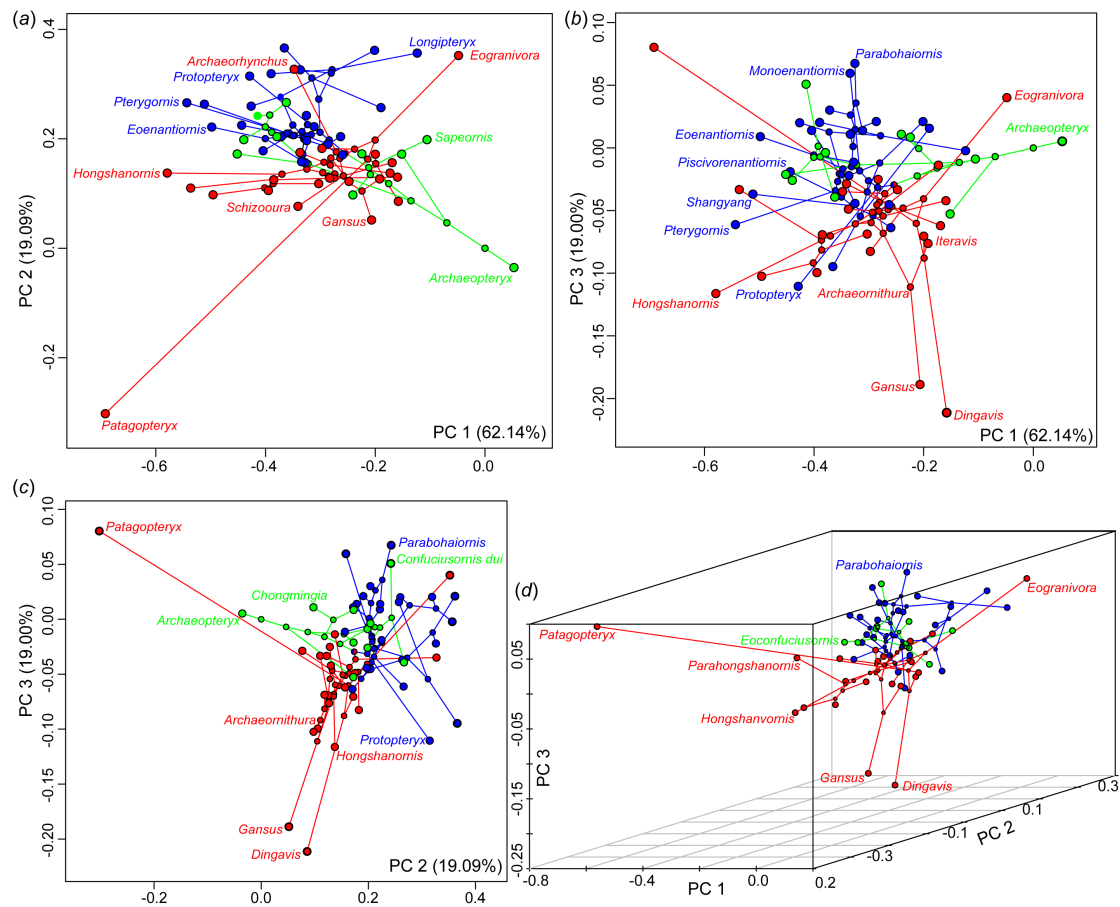


Figure S5. Phylomorphospace of Mesozoic birds defined by limb proportions. The phylogenetic backbone is derived from the “equal”-scaled strict consensus tree. (a–d) Binary and three-dimensional plots of PC1–3 recovered from pPCA. The color scheme repeats that of figure 2.

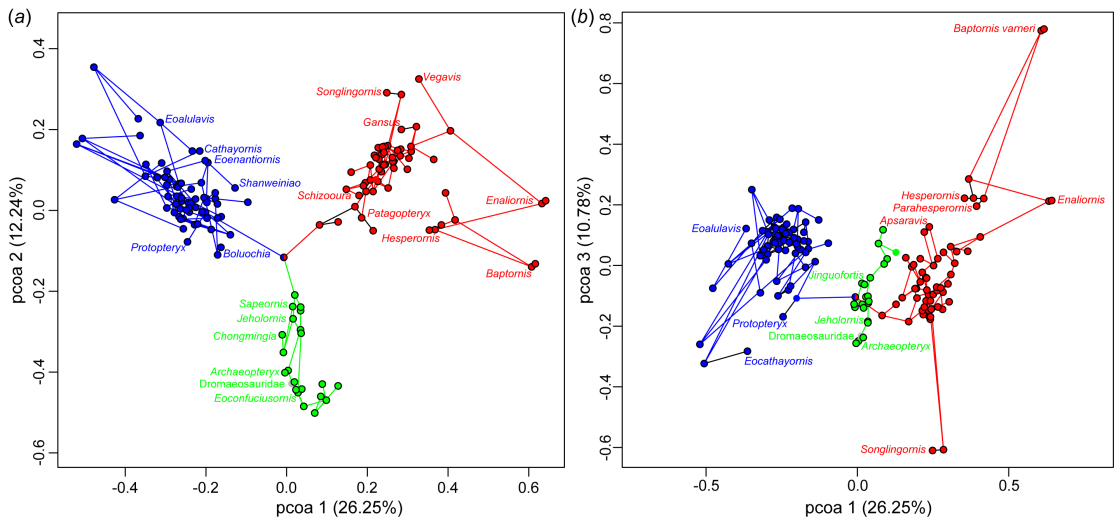


Figure S6. Phylomorphospace of Mesozoic birds defined by limb proportions using the tip-dating phylogeny. (a,b) Pairwise binary plots of PC 1–3 recovered from pPCA. The color scheme repeats that of figure 2.

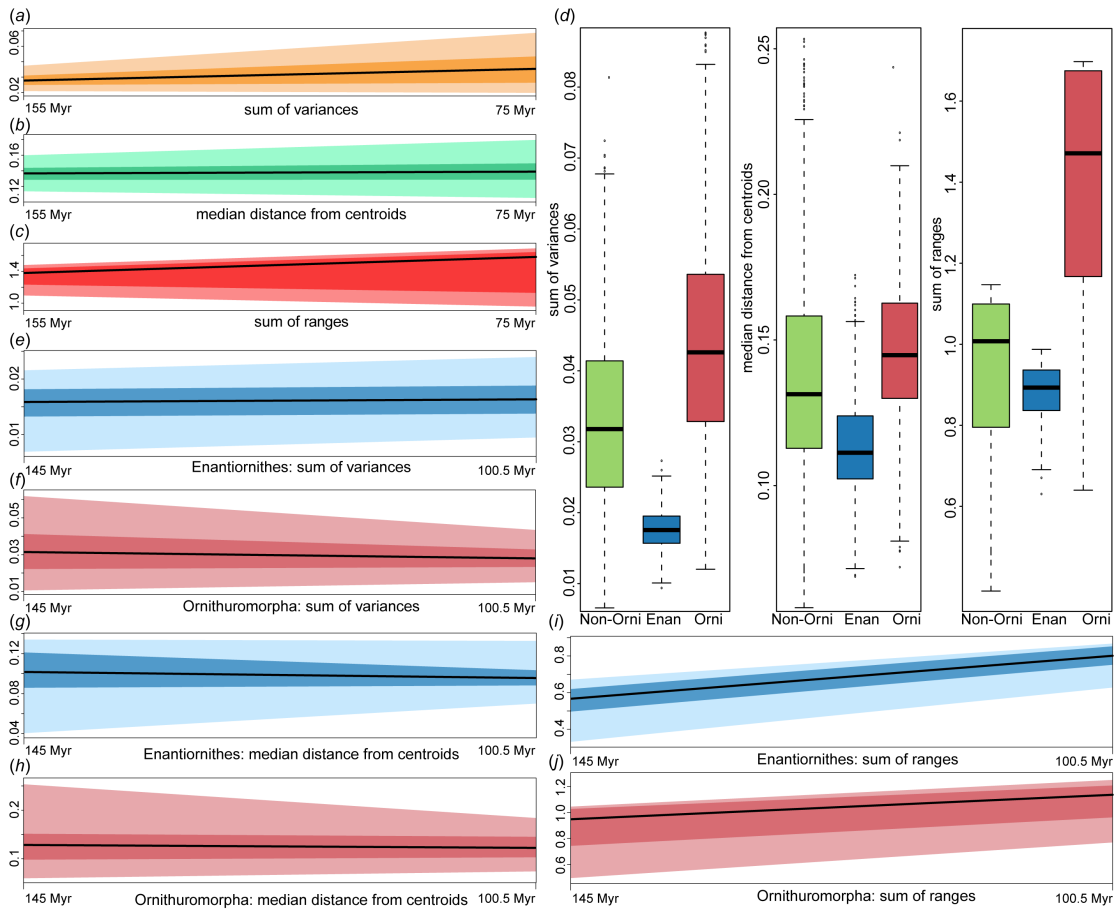


Figure S7. Disparity of Mesozoic birds in limb proportion. The phylogenetic backbone is derived from the “equal”-scaled strict consensus tree. (a–c) Disparity curves of Mesozoic birds across two equal-length time bins as defined in figure 3; (d) box plot showing disparity metrics among Mesozoic avian groups; (e–j) comparison of disparity between Enantiornithes and Ornithuromorpha during the Early Cretaceous in two equal-length time bins as defined in figure 3. The dark and light shadows indicate the 50% and 95% confidence intervals derived from bootstrap analyses, respectively.

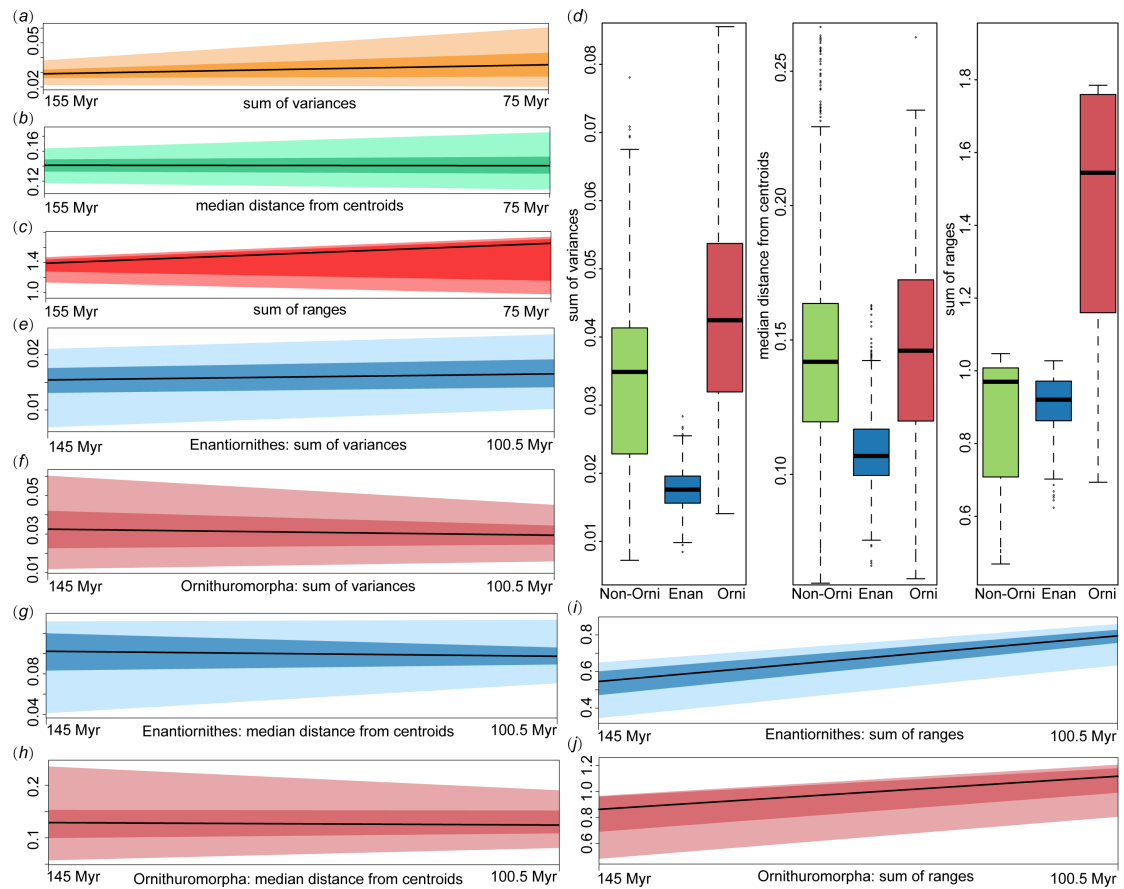


Figure S8. Disparity of Mesozoic birds in limb proportion using the tip-dating phylogeny. (a–c) Disparity curves of Mesozoic birds across two equal-length time bins as defined in figure 3; (d) box plot showing disparity metrics among Mesozoic avian groups; (e–j) comparison of disparity between Enantiornithes and Ornithuromorpha during the Early Cretaceous in two equal-length time bins as defined in figure 3. The dark and light shadows indicate the 50% and 95% confidence intervals derived from bootstrap analyses, respectively.

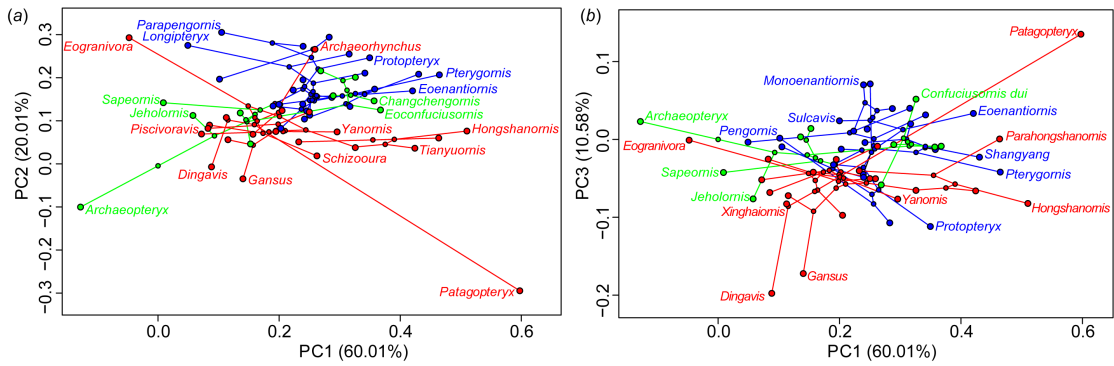


Figure S9. Bauplan phylomorphospace of Mesozoic birds using the tip-dating phylogeny with ancestral nodes. (a,b) Pairwise binary plots of PC 1–3 recovered from pPCA. The color scheme repeats that of figure 2.

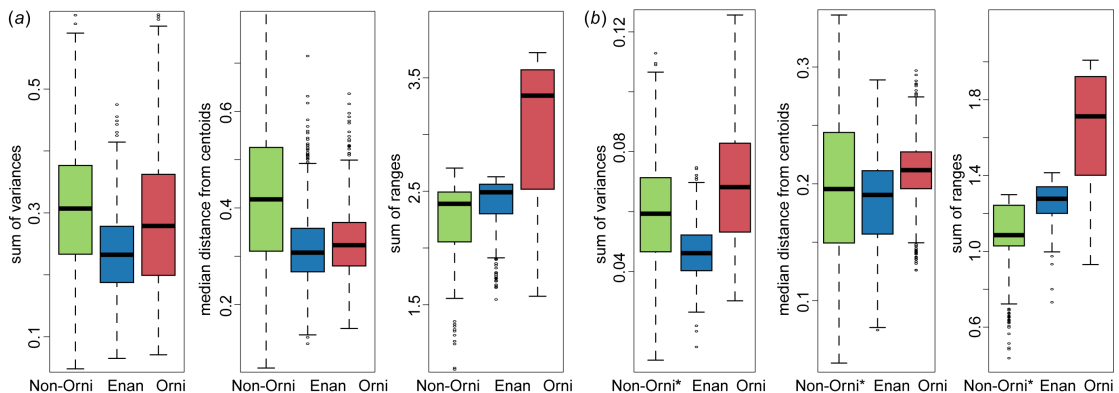


Figure S10. Box plots showing limb proportion disparity of Mesozoic birds with the ancestral state estimated using the lambda method. The phylogenetic backbone is derived from the “mbl”-scaled strict consensus tree. Three disparity metrics are shown: sum of variances, median distance from centroids, and sum of ranges. (a) All Mesozoic birds; (b) with the non-ornithothoracine *Sapeornis* excluded.

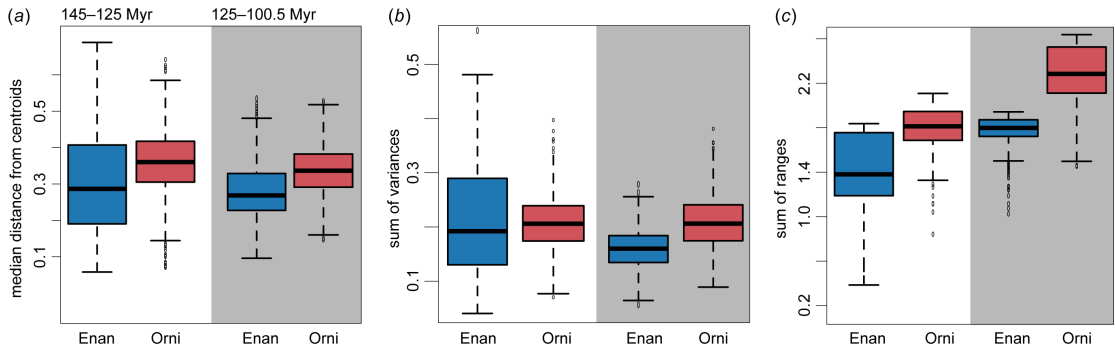


Figure S11. Comparison of limb proportion disparity between Early Cretaceous Enantiornithes and Ornithuromorpha with the ancestral state estimated using the lambda method. The phylogenetic backbone is derived from the “mbl”-scaled strict consensus tree. Three disparity metrics are shown: sum of variances, median distance from centroids. (a–c) Box plot showing disparity metrics across two equal-length time bins as defined in figure 3.

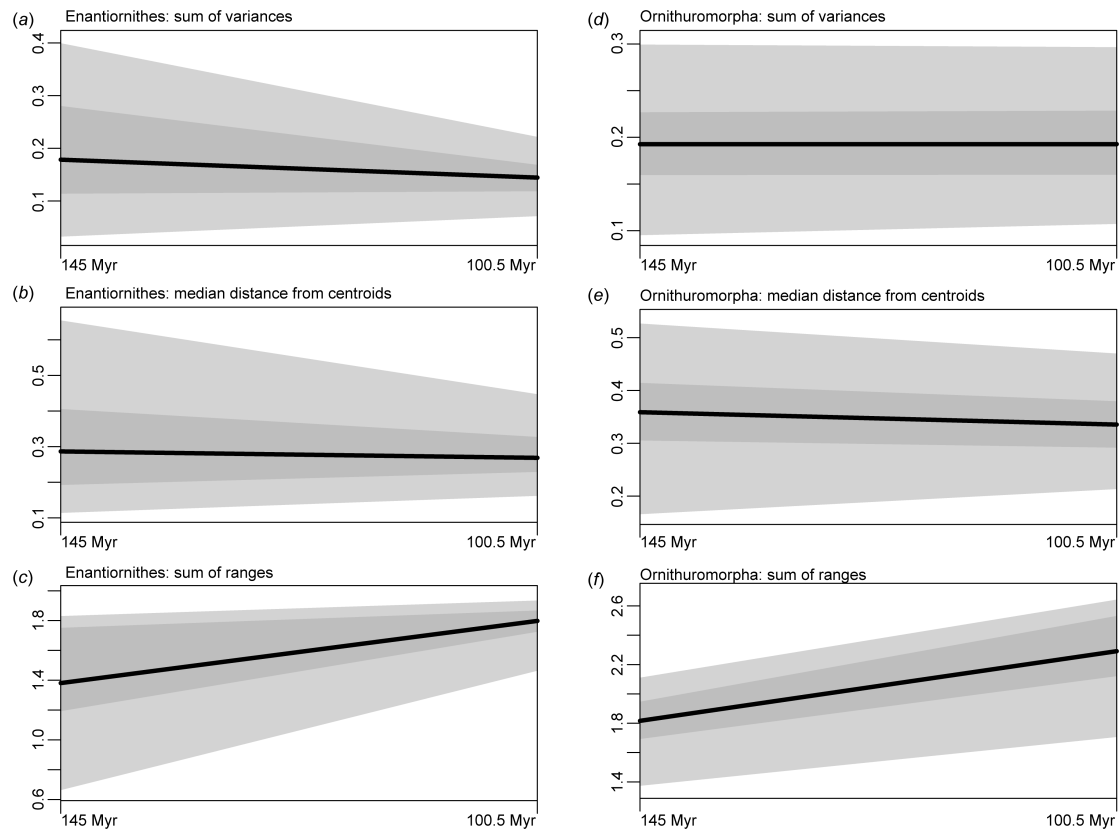


Figure S12. Comparison of limb proportion disparity between Early Cretaceous Enantiornithes and Ornithuromorpha with the ancestral states estimated using the lambda method. The phylogenetic backbone is derived from the “mbl”-scaled strict consensus tree. Three disparity metrics are shown: sum of variances, median distance from centroids. (a–f) Disparity curves across two equal-length time bins as defined in figure 3. The dark and light shadows indicate the 50% and 95% confidence intervals derived from bootstrap analyses, respectively.

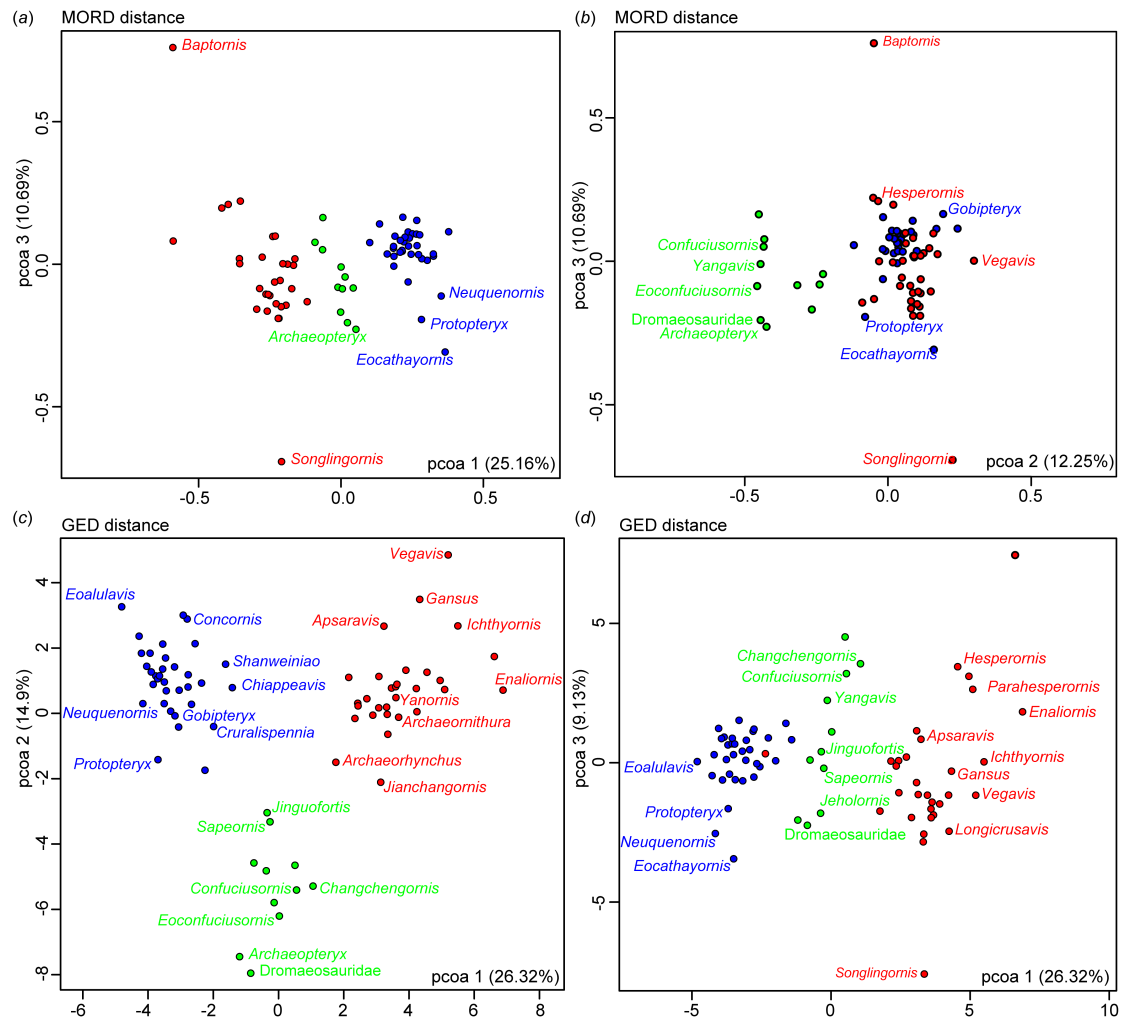


Figure S13. Discrete character morphospace of Mesozoic birds based on the “mbl”-scaled phylogeny. (a,b) Pairwise binary plots of pcoas 1–3 using MORD as the distance metrics; (c,d) pairwise binary plots of pcoas 1–3 using GED as the distance metrics. The color scheme repeats that of figure 2.

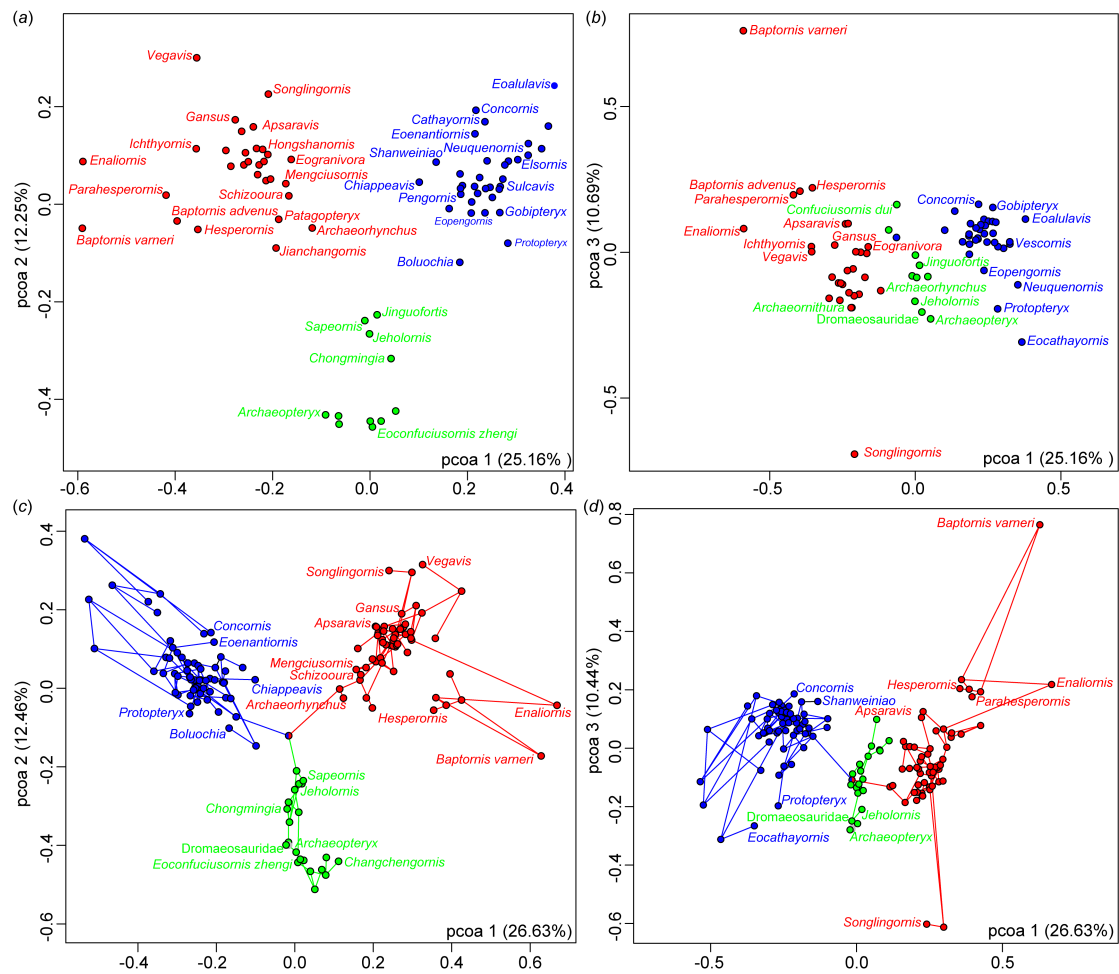


Figure S14. Discrete character morphospace of Mesozoic birds using the tip-dated phylogeny. MORD was used as the distance metrics. (a,b) Pairwise binary plots of pcoas 1–3 without ancestral nodes; (c,d) Pairwise binary plots of pcoas 1–3 with ancestral nodes. The color scheme repeats that of figure 2.

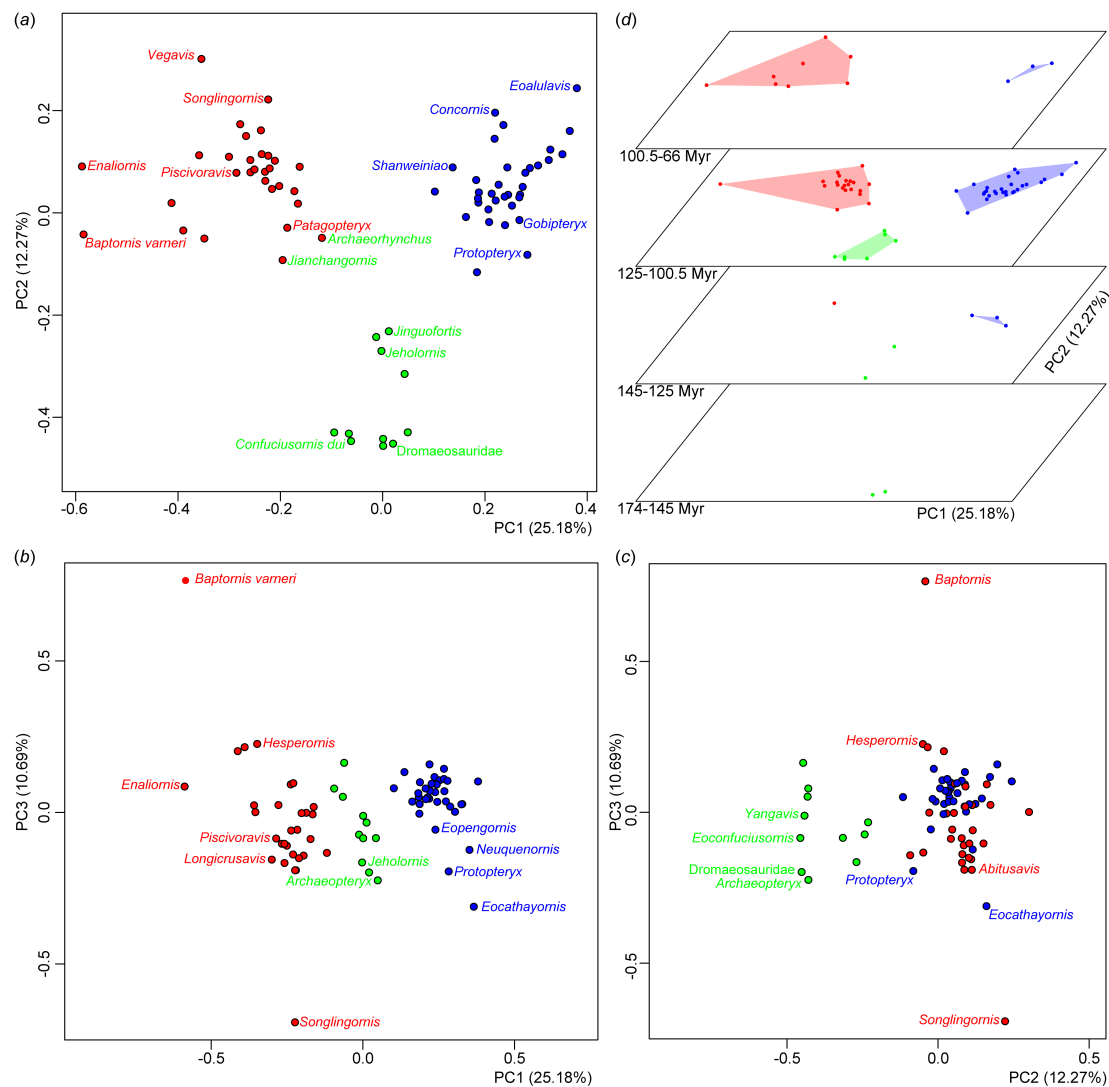


Figure S15. Discrete character morphospace of Mesozoic birds using “HSJ” method to calculate the distance metrics. The phylogenetic backbone is derived from “mbl”-scaled strict consensus tree. (a–c) Pairwise binary plots of pcoas 1–3 using “HSJ” method as the distance metrics; (d) binary plot of pcoas 1 and 2 stacked from the Late Jurassic to Cretaceous showing the changes of morphospace occupations. The color scheme repeats that of figure 2.

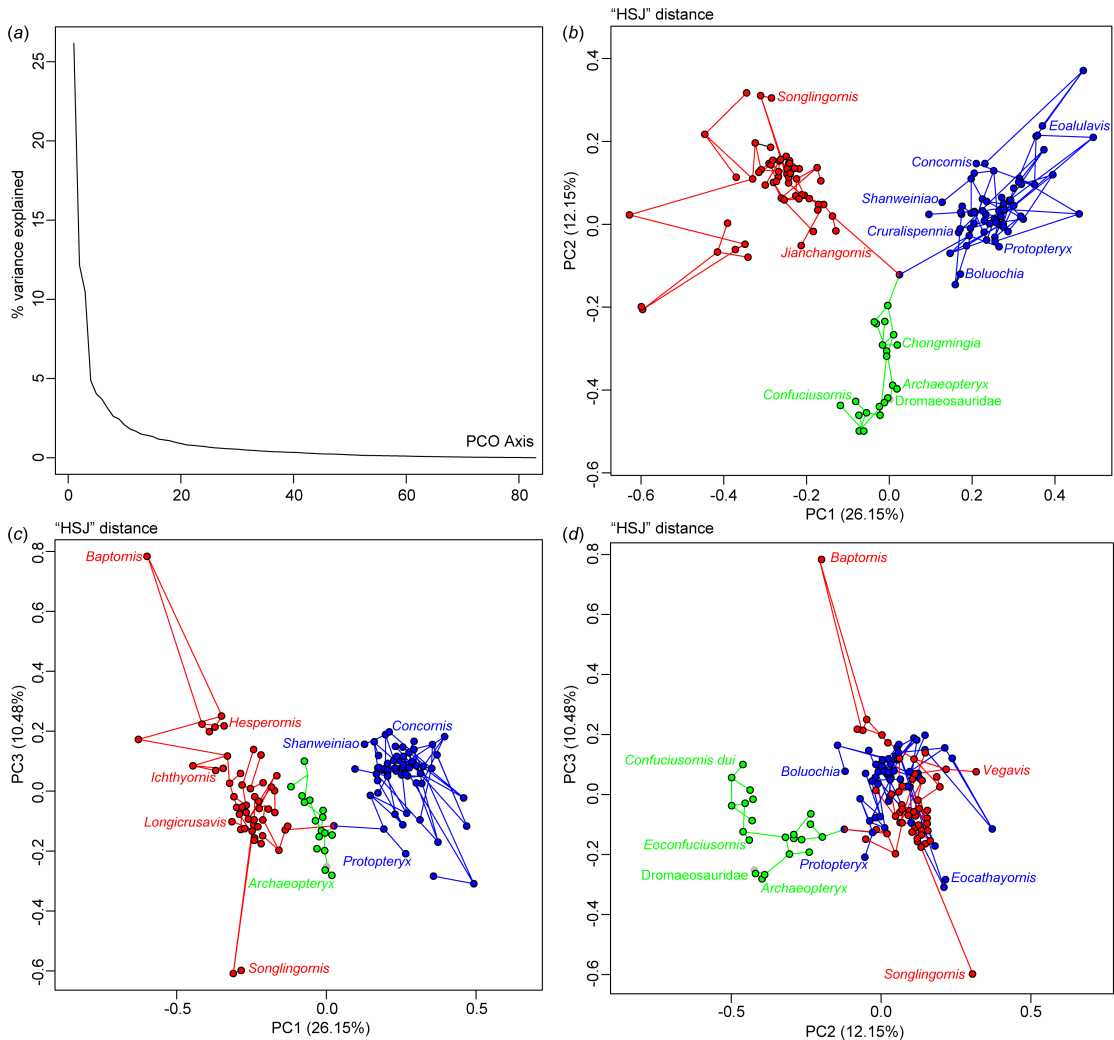


Figure S16. Discrete character morphospace of Mesozoic birds using “HSJ” method

to calculate the distance metrics. The phylogenetic backbone is derived from “mbl”-scaled strict consensus tree. (a–c) Pairwise binary plots of pcoas 1–3 using “HSJ” method as the distance metrics; (d) binary plot of pcoas 1 and 2 stacked from the Late Jurassic to Cretaceous showing the changes of morphospace occupations. The color scheme repeats that of figure 2.

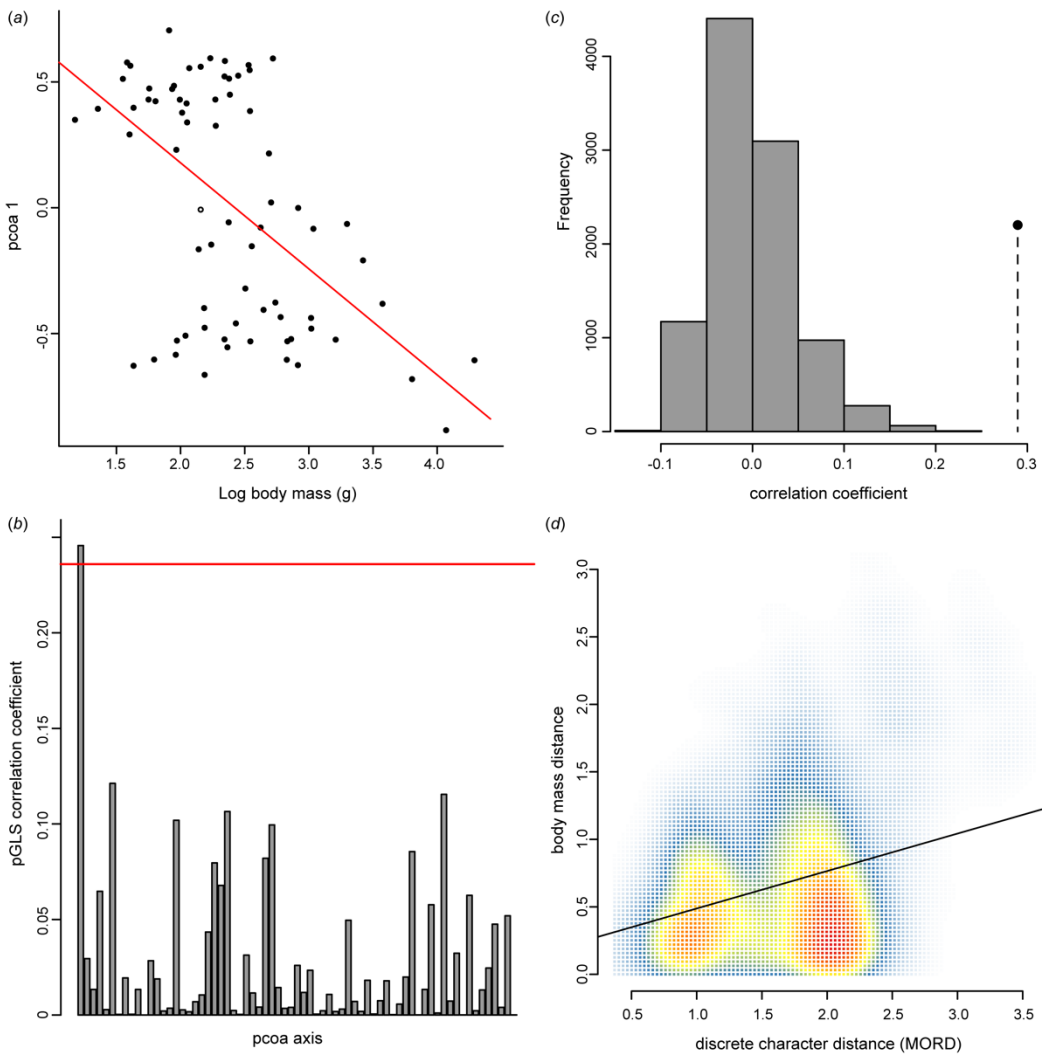


Figure S17. Results of correlation analyses of body mass and discrete character distance matrices. (a) Plot of first principal component axis (pcoa 1) against body mass; (b) bar plots of the correlation coefficients of body mass against each pcoa under phylogenetic least-squares (pGLS) model. The red line denotes the two-tailed 95% confidence interval; (c) histogram plot of the correlation of the permuted body mass and discrete character distance matrices (MORD method), with the observed correlation denoted by the dashed line; (d) Kernel density plot of discrete character distance matrices against body mass. The black line denotes the linear regression line.

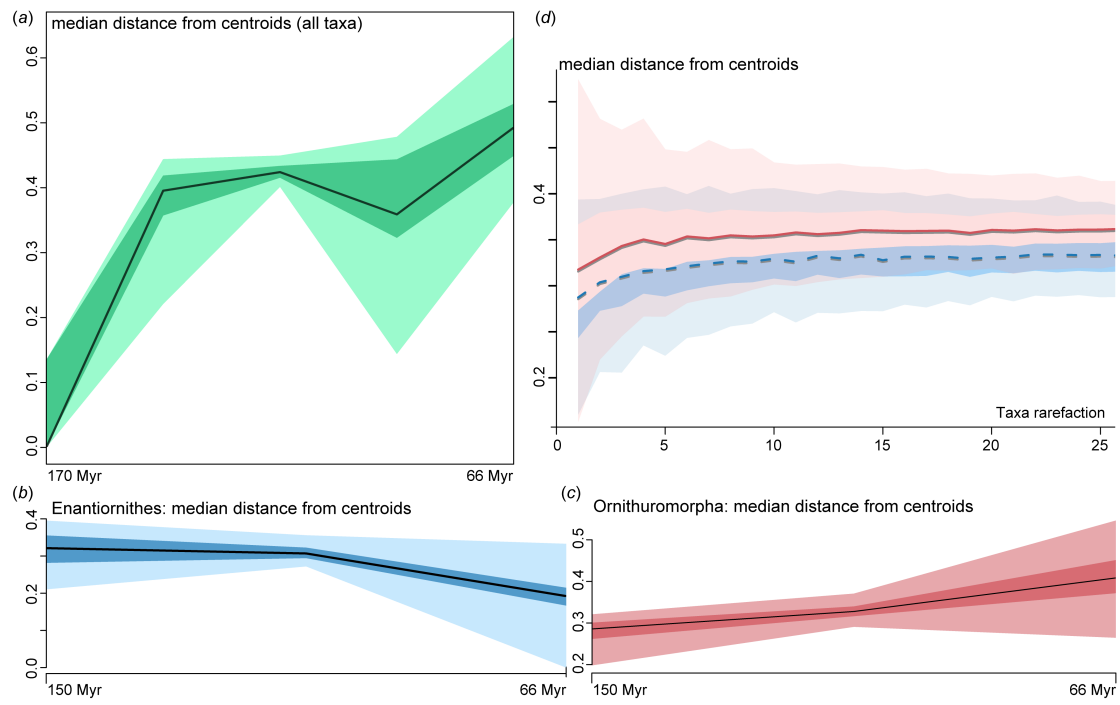


Figure S18. Morphological disparity of Mesozoic birds quantified by median distance from centroid. The phylogenetic backbone is the “mbl”-scaled phylogeny, and MORD was used as the distance metrics. (a) Disparity curves of Mesozoic birds as a whole across five time bins as defined in figure 5; (b,c) comparison between Enantiornithes and Ornithuromorpha across three subequal-length time bins as defined in figure 5; (d,e) rarefaction of disparity curves of Ornithuromorpha (in red) and Enantiornithes (in blue) showing that the results are not strongly affected by sampling bias. The dark and light shadows indicate the 50% and 95% confidence intervals derived from bootstrap analyses, respectively.

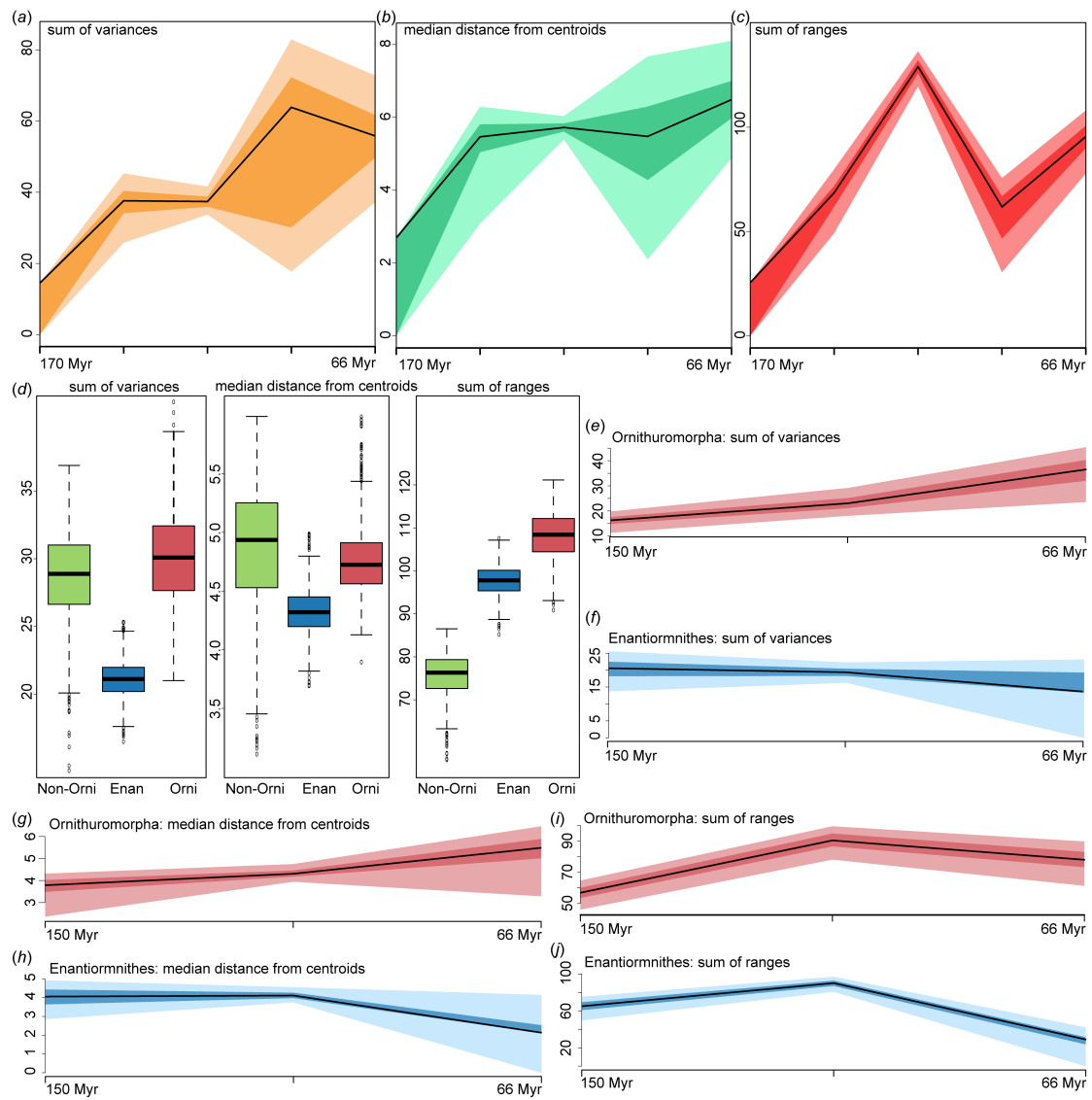


Figure S19. Morphological disparity of Mesozoic birds using the GED as the distance metric. The phylogenetic backbone is the “mbl”-scaled phylogeny. (a–c) Disparity curves of Mesozoic birds as a whole across five time bins as defined in figure 5; (d) box plot showing disparity metrics of Mesozoic avian groups; (e–j) Disparity curves of Enantiornithes and Ornithuromorpha across three subequal-length time bins as defined in figure 5. The dark and light shadows indicate the 50% and 95% confidence intervals derived from bootstrap analyses, respectively.

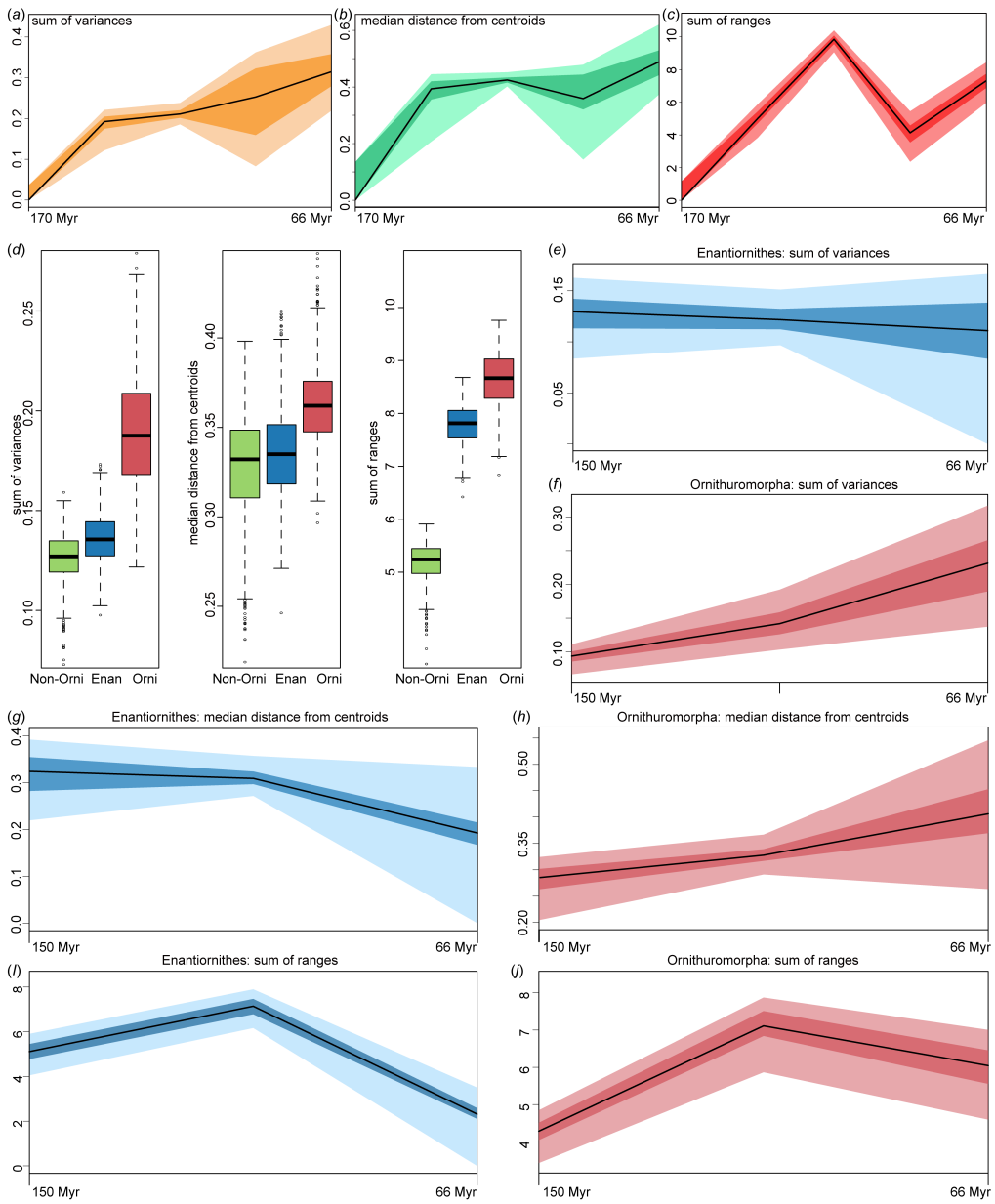


Figure S20. Morphological disparity of Mesozoic birds using the tip-dated phylogeny without ancestral nodes. The MORD was used as the distance metrics. (a–c) Disparity curves of Mesozoic birds as a whole across five time bins as defined in figure 5; (d) box plot showing disparity metrics of Mesozoic avian groups; (e–j) disparity curves of Enantiornithes and Ornithuromorpha across three subequal-length time bins as defined in figure 5. The dark and light shadows indicate the 50% and 95% confidence intervals derived from bootstrap analyses, respectively.

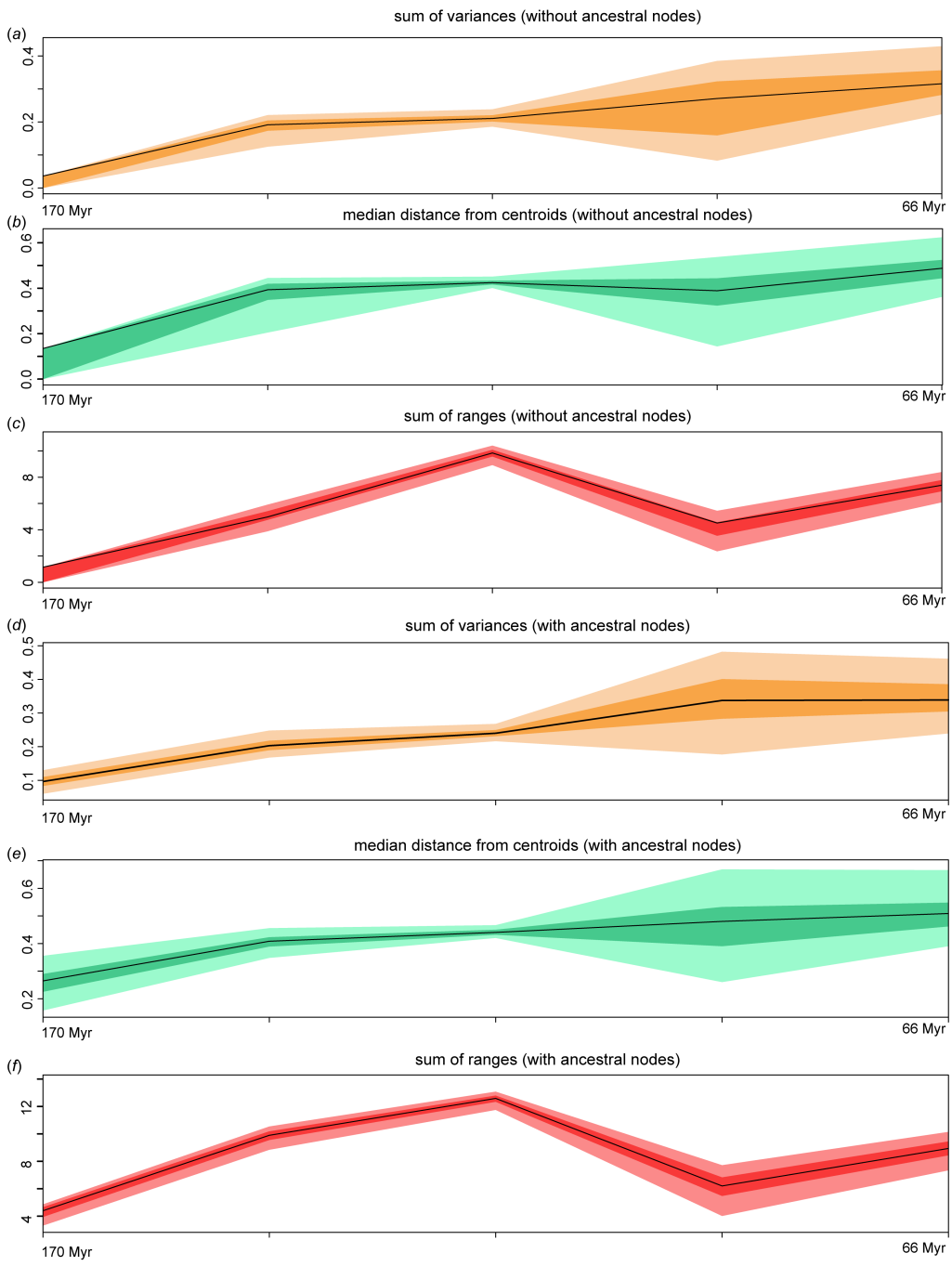


Figure S21. Morphological disparity of Mesozoic birds. The phylogenetic backbone is the “equal”-scaled phylogeny, and MORD was used as the distance metrics. Disparity curves of Mesozoic birds without (a–c) and with ancestral nodes (e–f) across five time bins as defined in figure 5. The dark and light shadows indicate the 50% and 95% confidence intervals derived from bootstrap analyses, respectively.

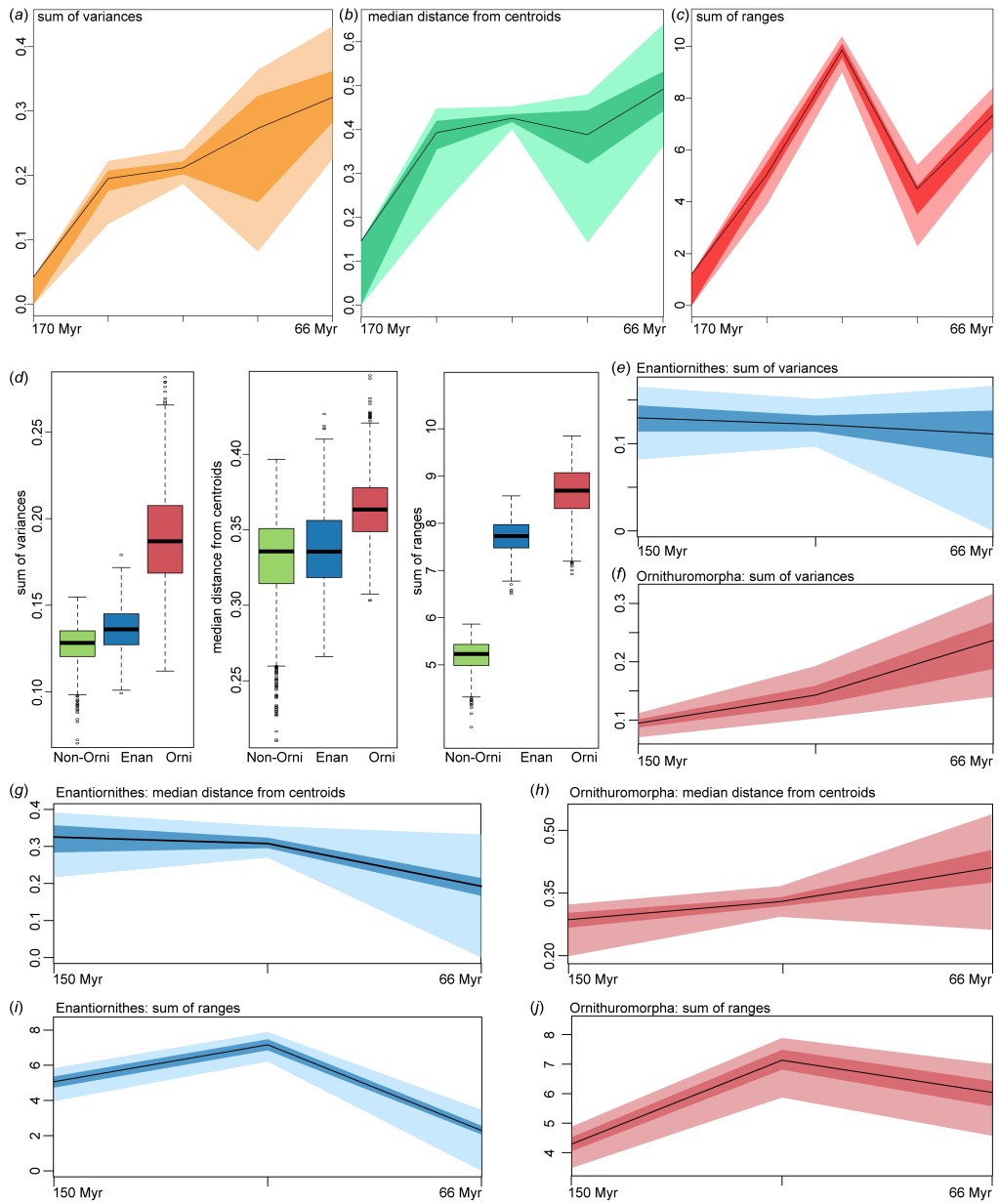


Figure S22. Morphological disparity of Mesozoic birds using “HSJ” method to calculate the distance metrics. The phylogenetic backbone is the “mbl”-scaled phylogeny. (a–c) Disparity curves of Mesozoic birds as a whole across five time bins as defined in figure 5; (d) box plot showing disparity metrics of Mesozoic avian groups; (e–j) disparity curves of Enantiornithes and Ornithuromorpha across three subequal-length time bins as defined in figure 5. The dark and light shadows indicate the 50% and 95% confidence intervals derived from bootstrap analyses, respectively.

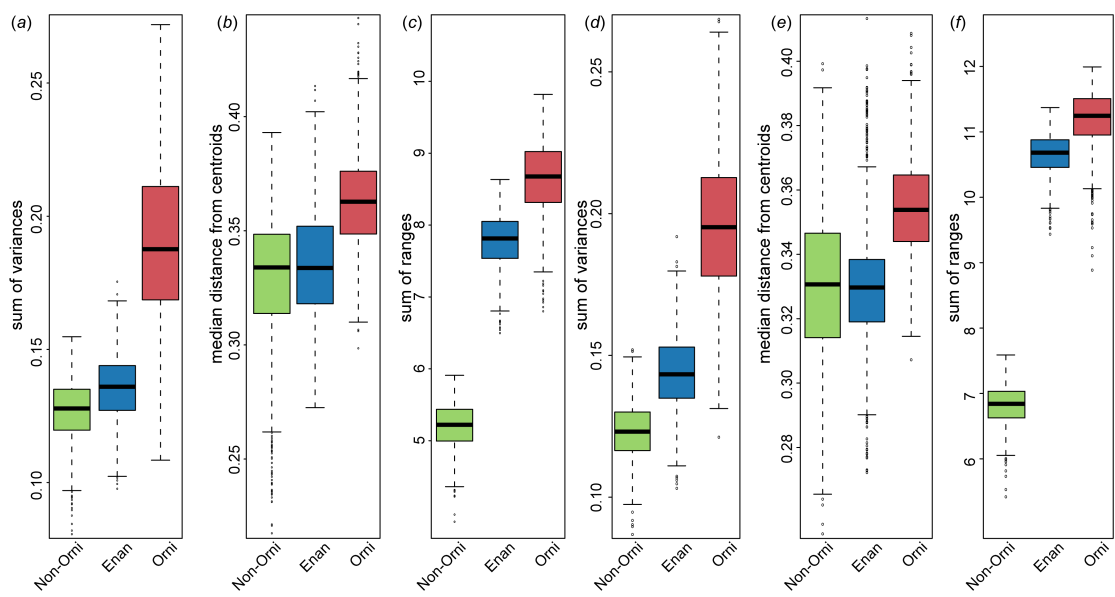


Figure S23. Box plots showing morphological disparity of Mesozoic birds. The phylogenetic backbone is the “equal”-scaled phylogeny, and MORD was used as the distance metrics. (a–c) Ancestral nodes excluded; (d–f) ancestral nodes included.

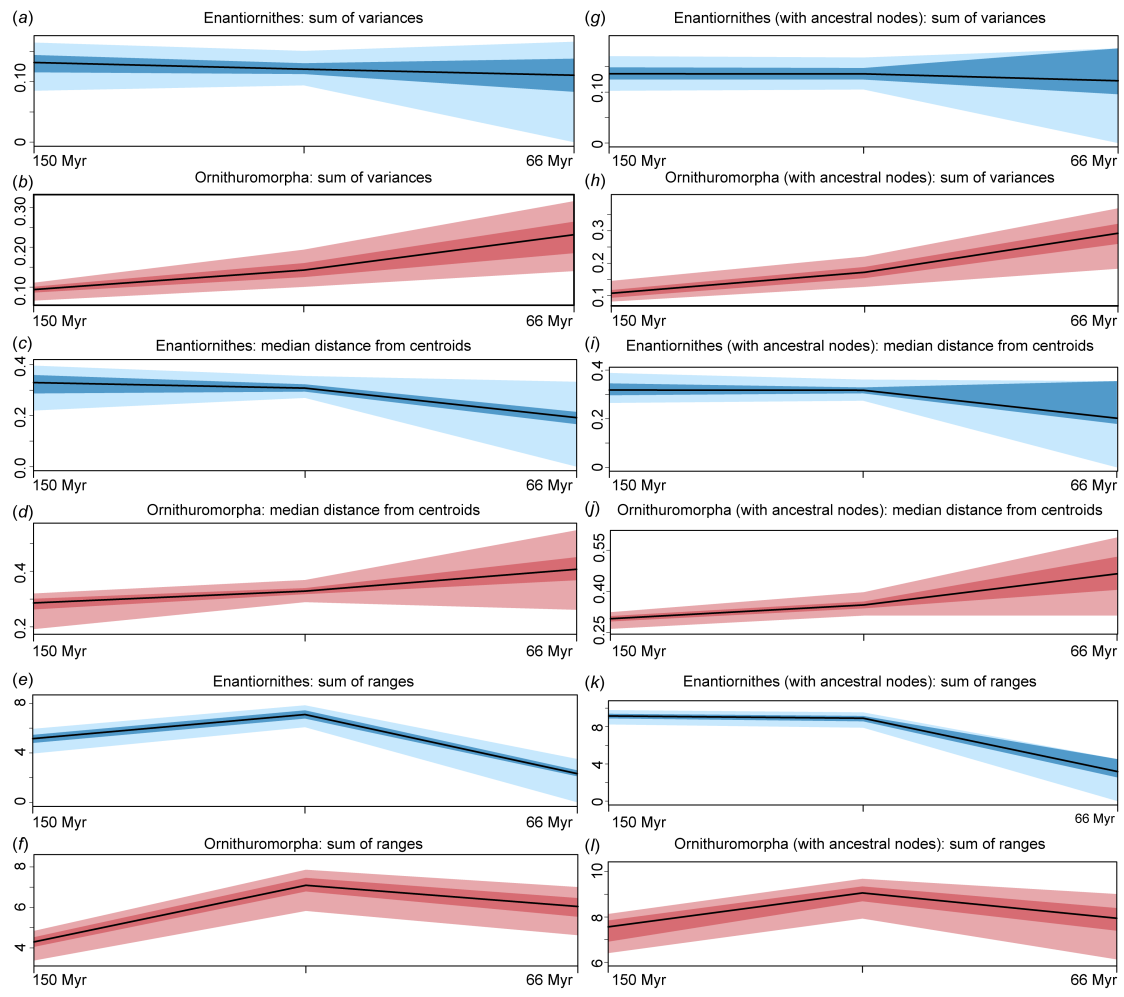


Figure S24. Comparison of morphological disparity between Enantiornithes and Ornithuromorpha. The phylogenetic backbone is the “equal”-scaled phylogeny, and MORD was used as the distance metrics. The disparity curves are binned into three subequal-length time bins as defined in figure 5. (a–f) Ancestral nodes excluded; (g–l) ancestral nodes included. The dark and light shadows indicate the 50% and 95% confidence intervals derived from bootstrap analyses, respectively.

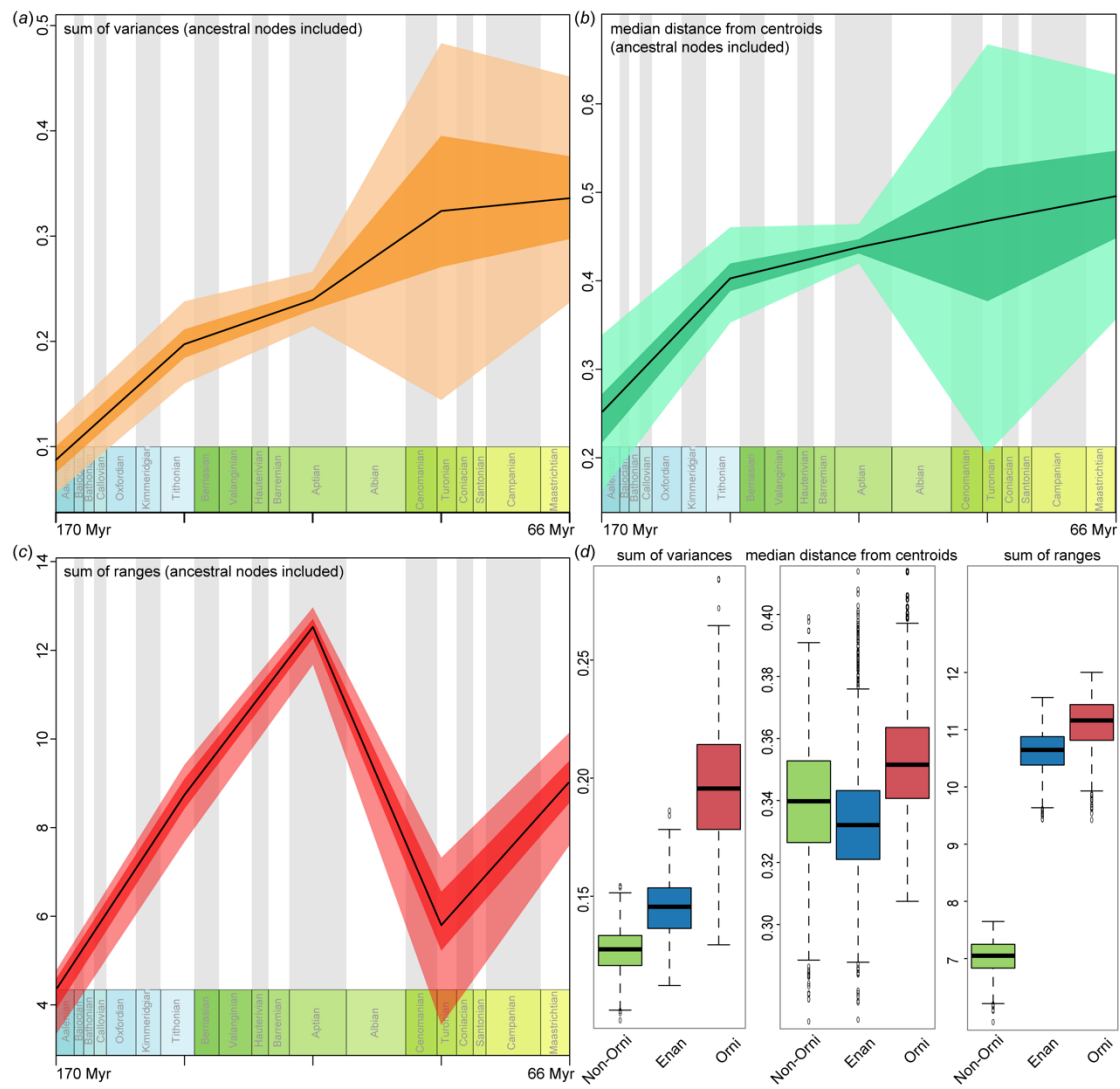


Figure S25. Morphological disparity of Mesozoic birds with ancestral nodes included.

The phylogenetic backbone is the “mbl”-scaled phylogeny, and MORD was used as the distance metrics. (a–c) Disparity curves of Mesozoic birds as a whole across five time bins as defined in figure 5; (d) box plot showing disparity metrics of Mesozoic avian groups. The dark and light shadows indicate the 50% and 95% confidence intervals derived from bootstrap analyses, respectively.

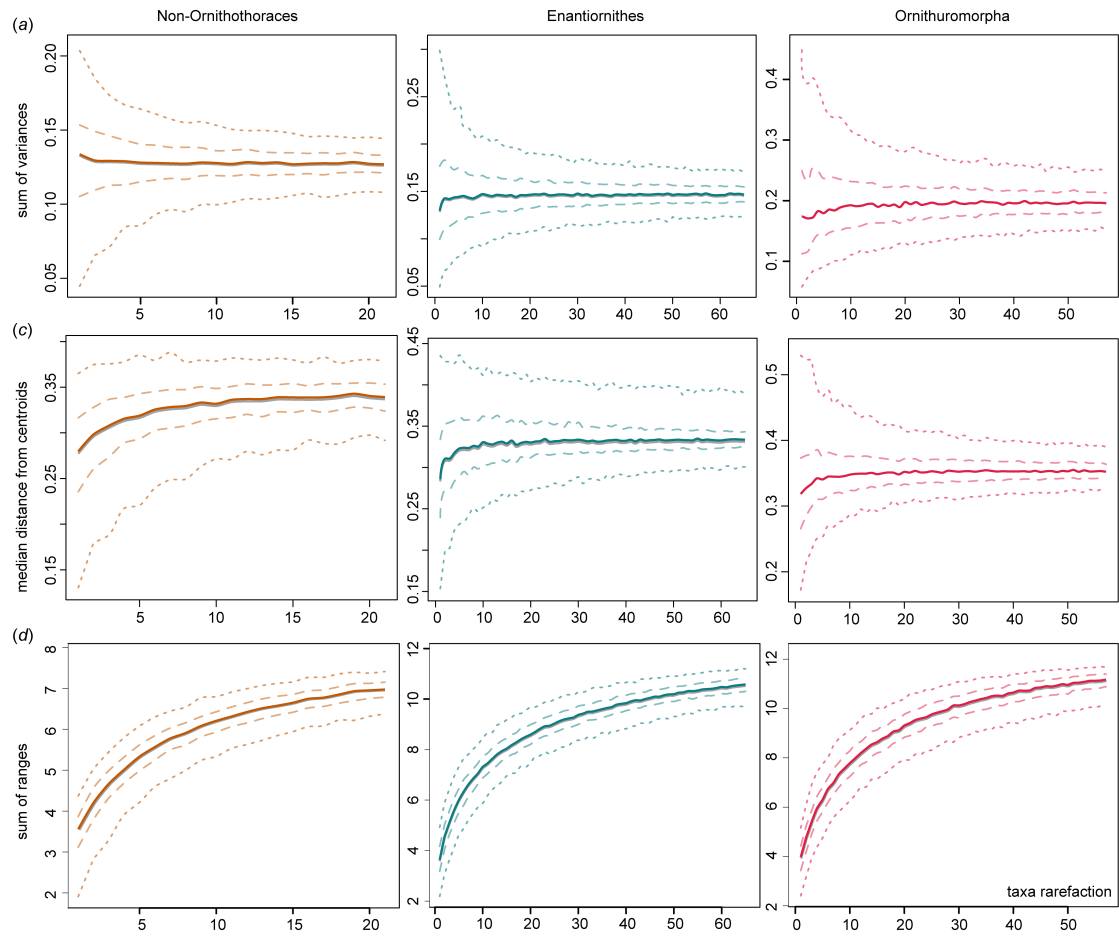


Figure S26. Rarefaction curves of Mesozoic birds with ancestral nodes included. The phylogenetic backbone is the “mbl”-scaled phylogeny, and MORD was used as the distance metrics. Three disparity metrics are shown: sum of variances (a), median distance from centroid (b), and sum of ranges (c). The results show that the main conclusion that Ornithuromorpha is more disparate than other avian groups is relatively robust to sampling bias.

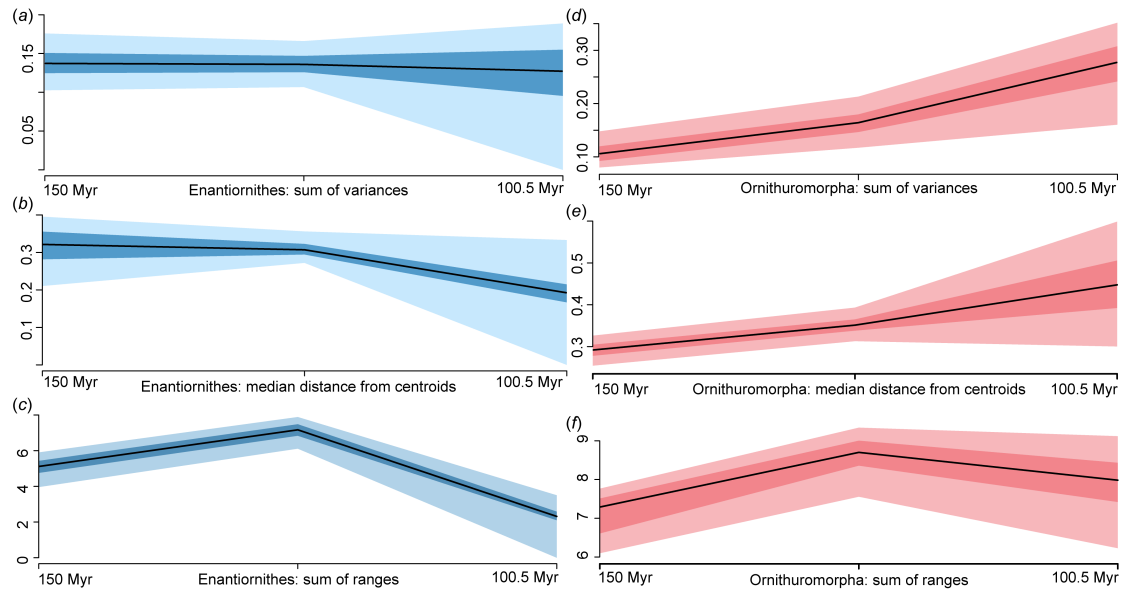


Figure S27. Comparison of morphological disparity between Enantiornithes and Ornithuromorpha with ancestral nodes included. The phylogenetic backbone is the “mbl”-scaled phylogeny, and MORD was used as the distance metrics. Three disparity metrics are shown: sum of variance (a,d), median distance from centroid (b,e), and sum of ranges (c,f). Disparity curves are binned into subequal-length time bins as defined in figure 5. The dark and light shadows indicate the 50% and 95% confidence intervals derived from bootstrap analyses, respectively.

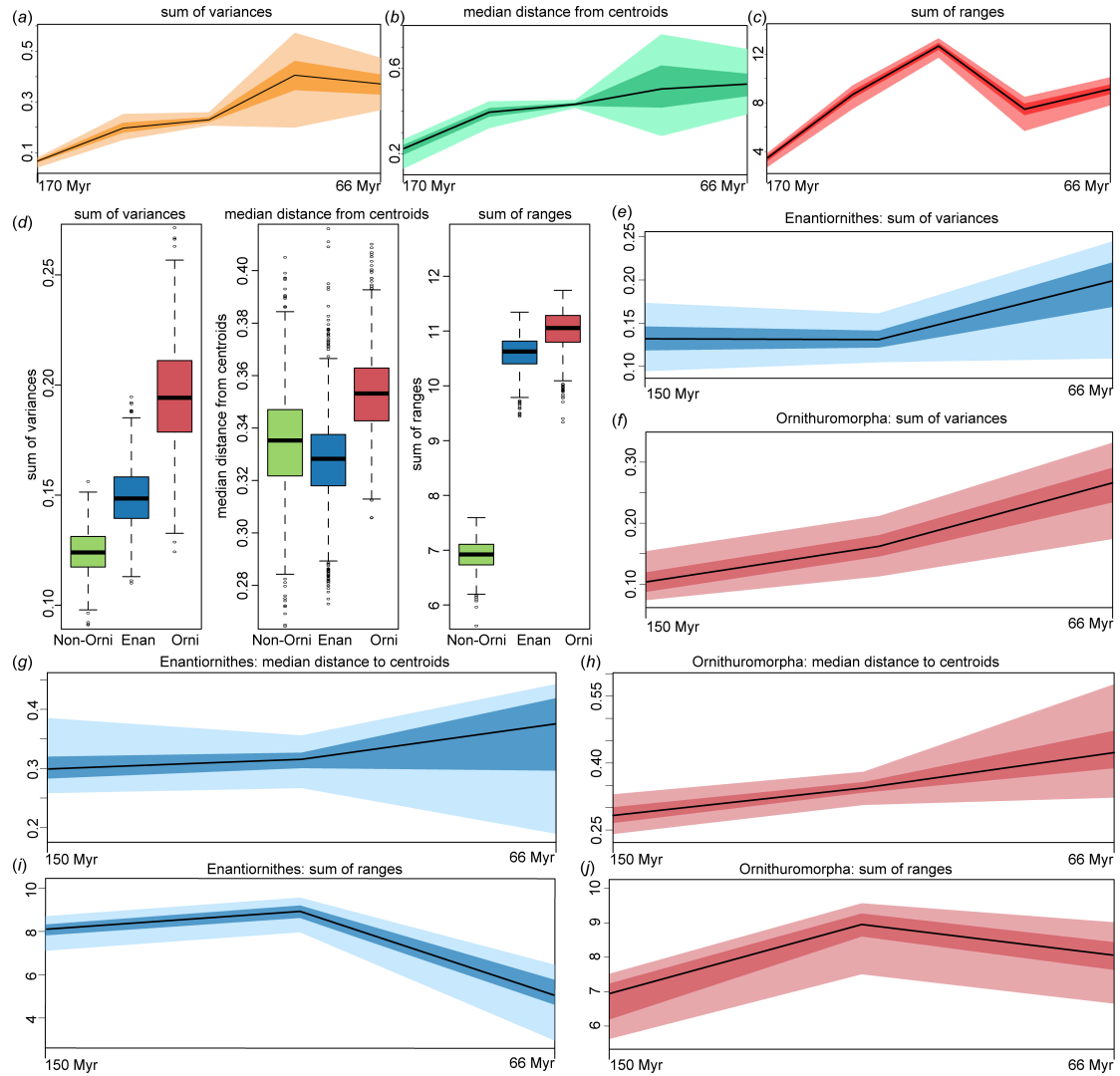


Figure S28. Morphological disparity of Mesozoic birds using the tip-dated phylogeny with ancestral nodes included. The MORD was used as the distance metrics. (a–c) Disparity curves of Mesozoic birds as a whole across five time bins as defined in figure 5; (d) box plot showing disparity metrics of Mesozoic avian groups; (e–j) disparity curves of Enantiornithes and Ornithuromorpha across three subequal-length time bins as defined in figure 5. The dark and light shadows indicate the 50% and 95% confidence intervals derived from bootstrap analyses, respectively.

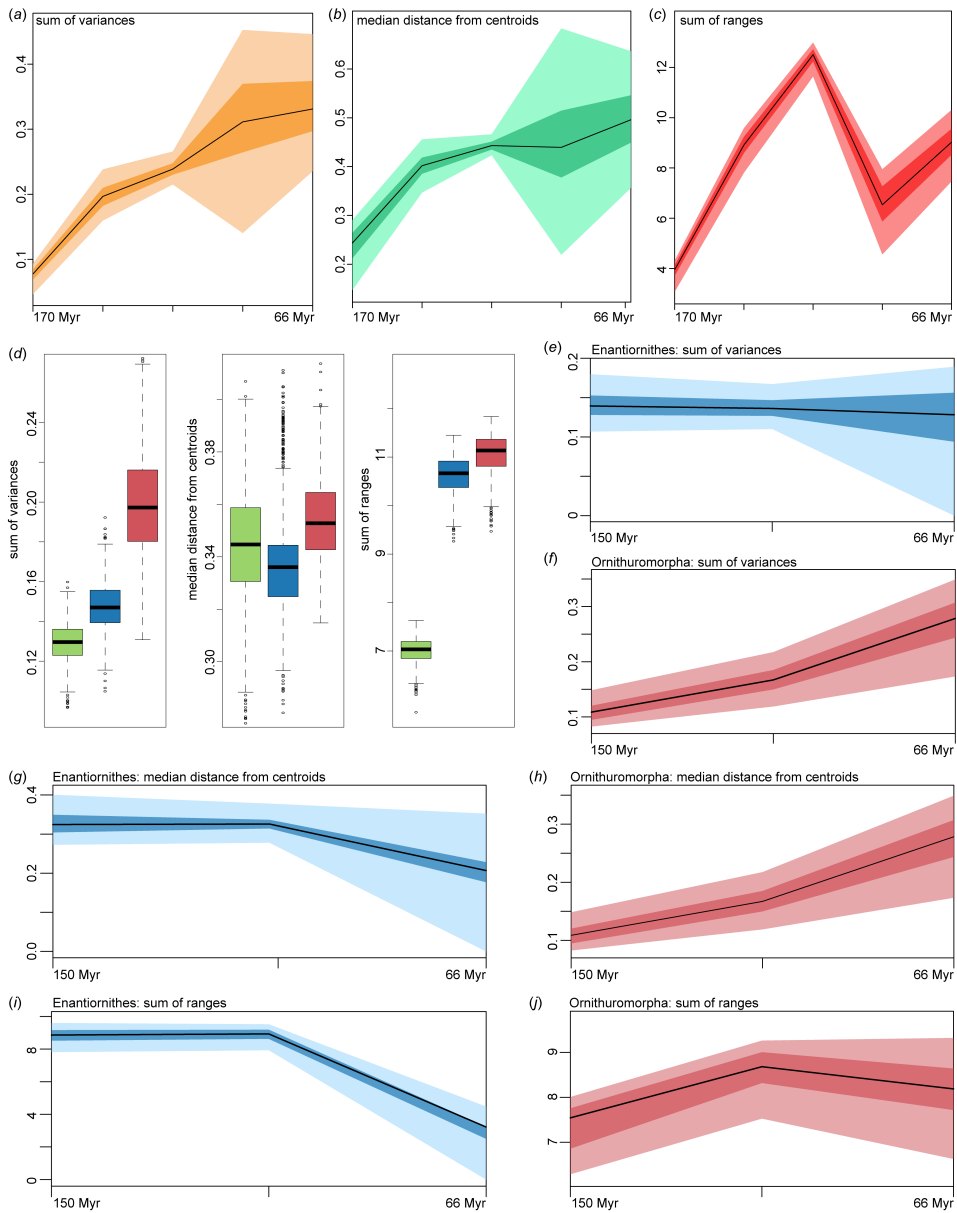


Figure S29. Morphological disparity of Mesozoic birds with ancestral states

estimated using the “HJS” method. The phylogenetic backbone is derived from “mbl”-scaled strict consensus tree. (a–c) Disparity curves of Mesozoic birds as a whole across five time bins as defined in figure 5; (d) box plot showing disparity metrics of Mesozoic avian groups; (e–j) disparity curves of Enantiornithes and Ornithuromorpha across three subequal-length time bins as defined in figure 5. The dark and light shadows indicate the 50% and 95% confidence intervals derived from bootstrap analyses, respectively.

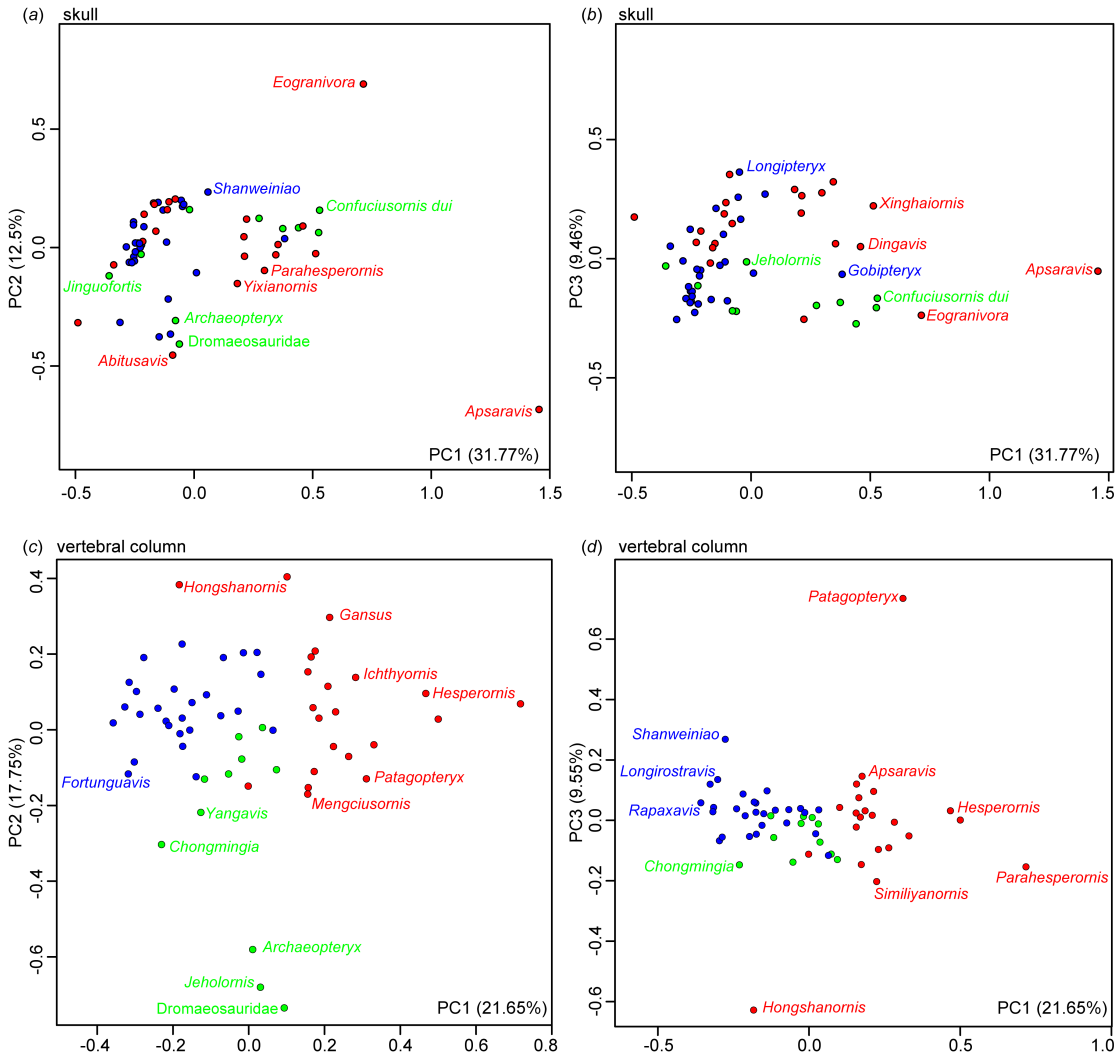


Figure S30. Discrete character morphospace of the skull and vertebral column of Mesozoic birds. The phylogenetic backbone is the “mbl”-scaled phylogeny, and MORD was used as the distance metrics. Pairwise binary plots of pcoas 1and 2 of the skull (a,b) and vertebral column (c,d). The color scheme repeats that of figure 2.

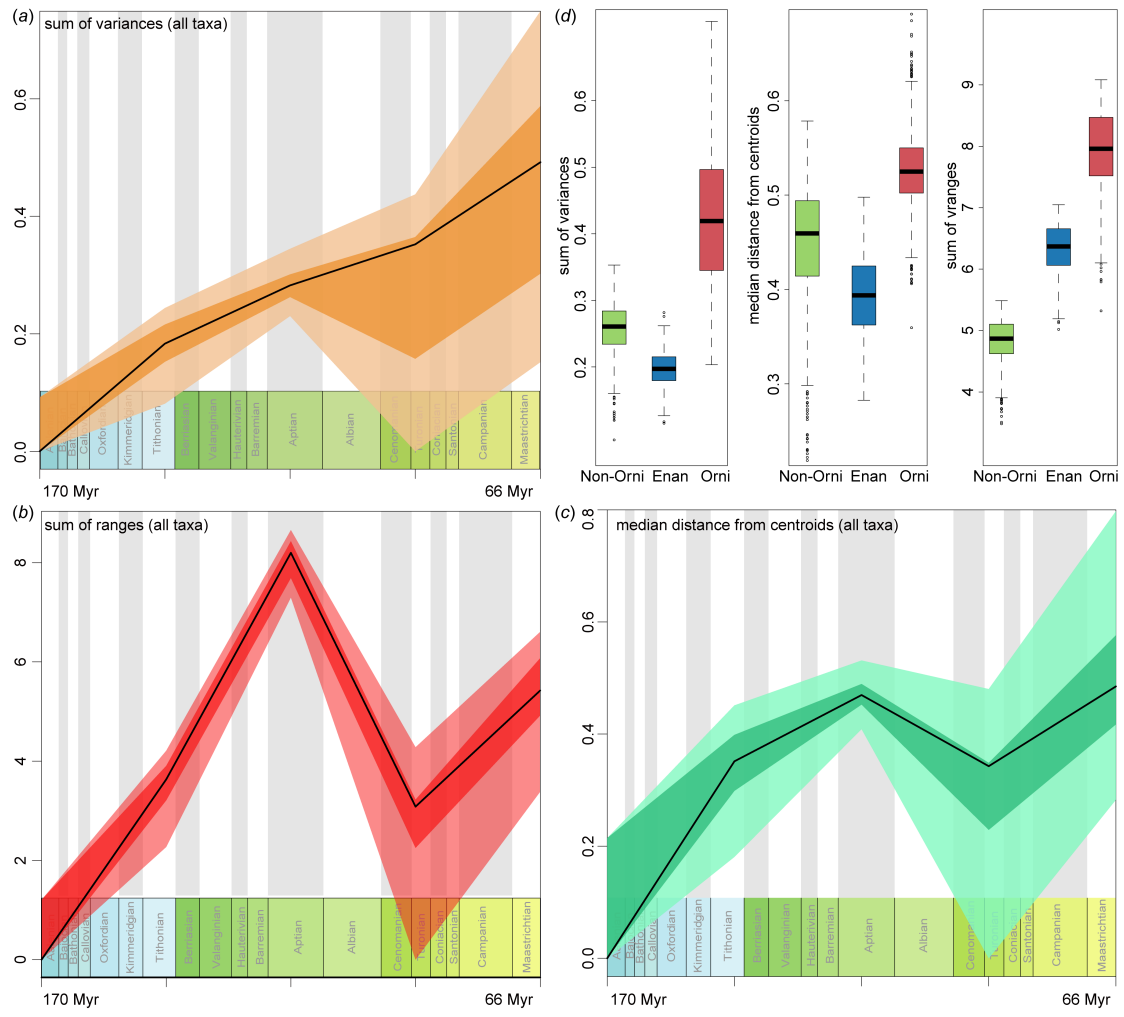


Figure S31. Morphological disparity of the skull of Mesozoic birds. The phylogenetic backbone is the “mbl”-scaled phylogeny, and MORD was used as the distance metrics. (a–c) Disparity curves of Mesozoic birds as a whole across five time bins as defined in figure 5; (d) box plot showing disparity metrics of Mesozoic avian groups. The dark and light shadows indicate the 50% and 95% confidence intervals derived from bootstrap analyses, respectively.

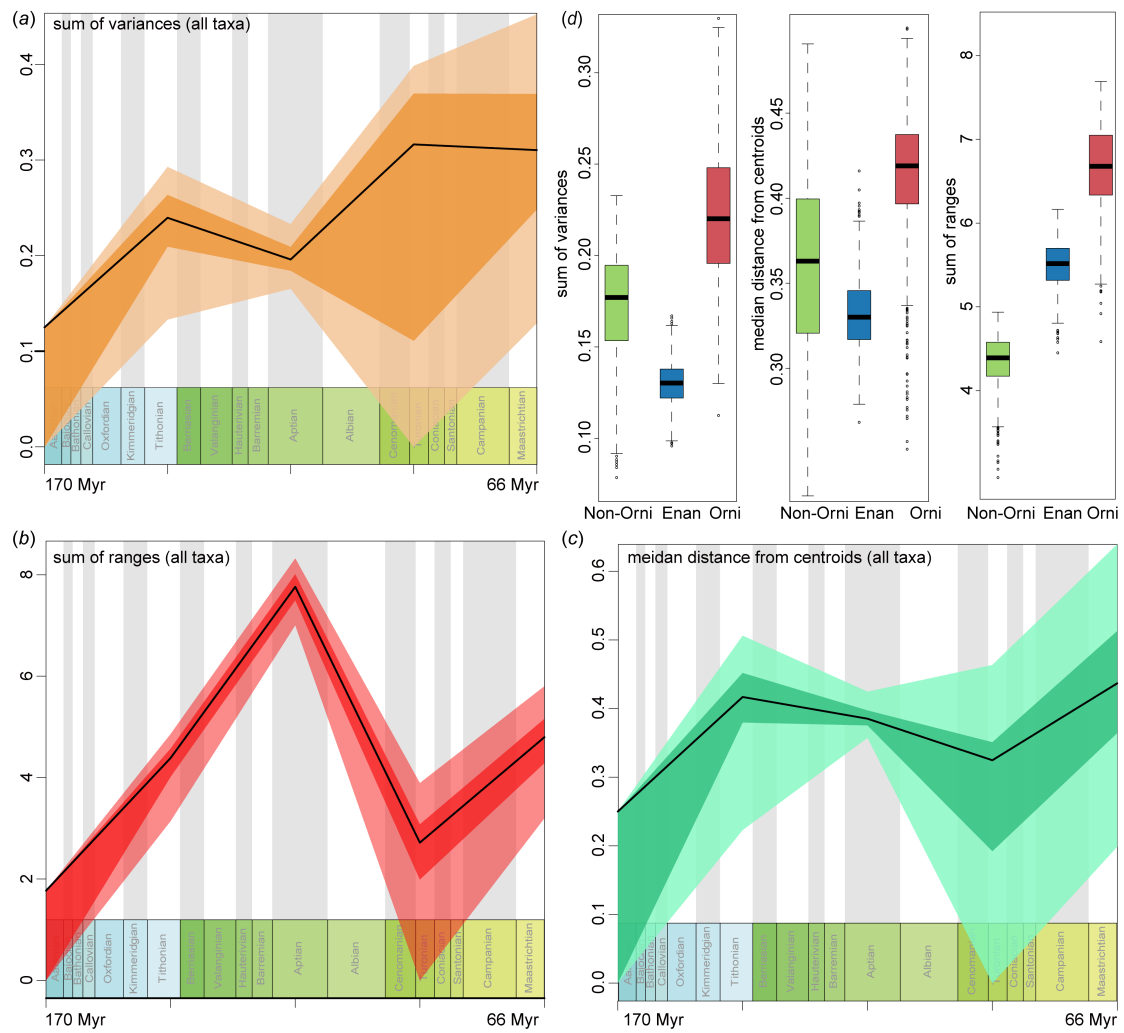


Figure S32. Morphological disparity of the vertebral column of Mesozoic birds. The phylogenetic backbone is the “mbl”-scaled phylogeny, and MORD was used as the distance metrics. (a–c) Disparity curves of Mesozoic birds as a whole across five time bins as defined in figure 5; (d) box plot showing disparity metrics of Mesozoic avian groups. The dark and light shadows indicate the 50% and 95% confidence intervals derived from bootstrap analyses, respectively.

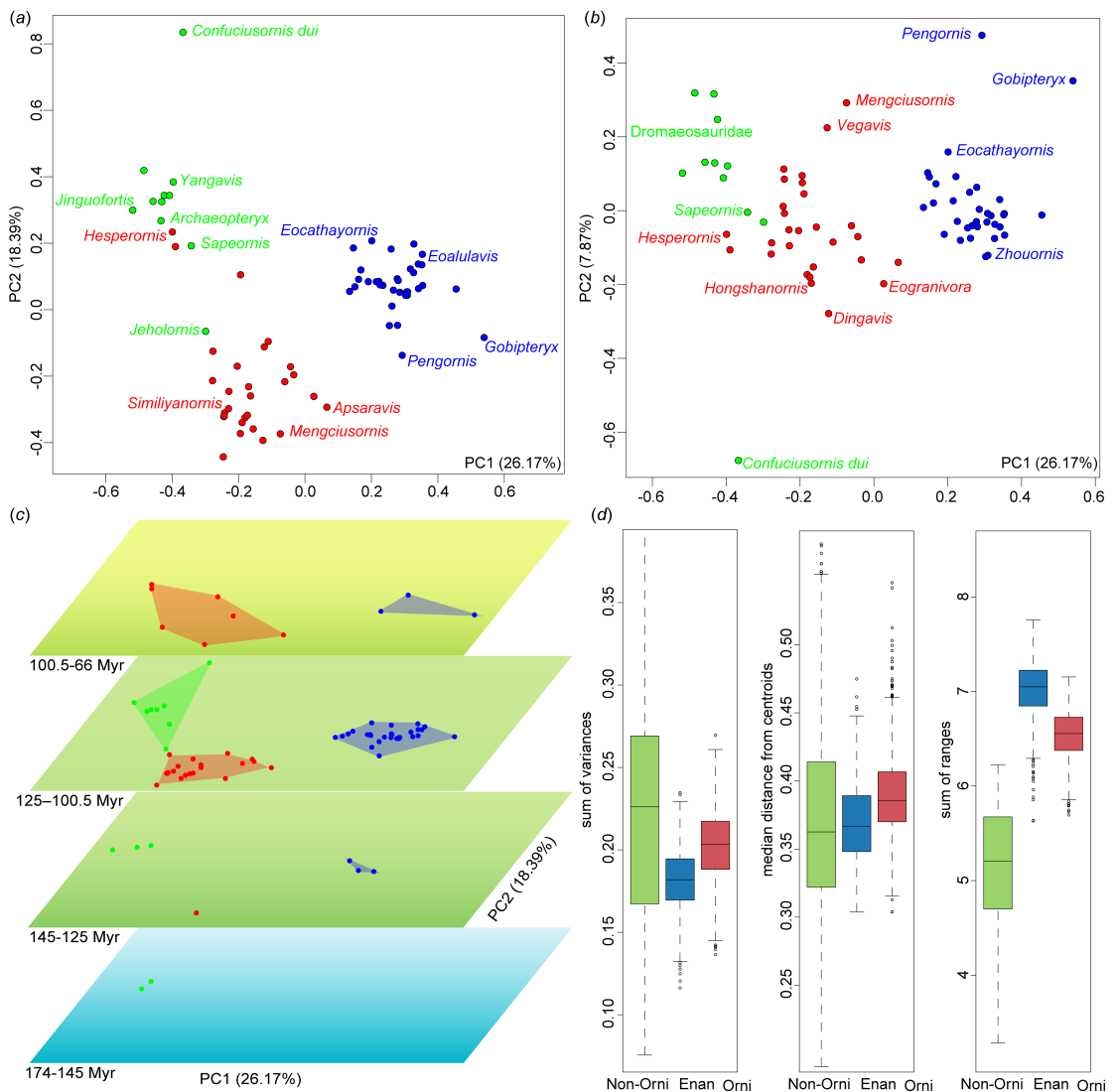


Figure S33. Discrete character morphospace of the pectoral girdle of Mesozoic birds.

The phylogenetic backbone is the “mbl”-scaled phylogeny, and MORD was used as the distance metrics. Pairwise binary plots of pcoas 1–3 (a,b), and (c) stacked from the Late Jurassic to Cretaceous showing the changes of morphospace occupations; (d) box plots showing disparity metrics among groups.

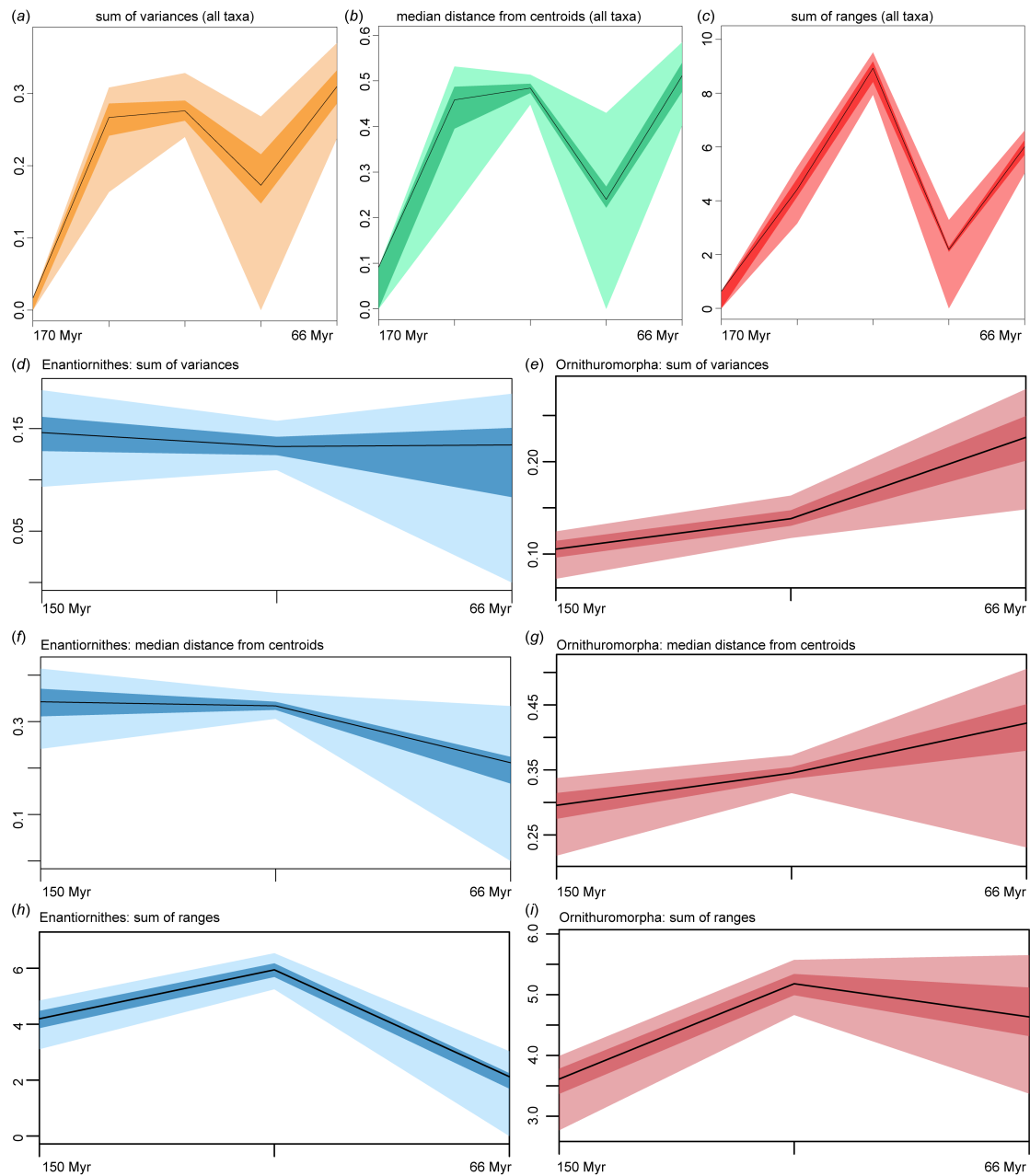


Figure S34. Morphological disparity of the pectoral girdle of Mesozoic birds. The phylogenetic backbone is derived from “mbl”-scaled strict consensus tree, and MORD was used as the distance metrics. (a–c) Disparity curves of Mesozoic birds as a whole across five time bins as defined in figure 5; (d–i) disparity curves of Enantiornithes and Ornithuromorpha across three subequal-length time bins as defined in figure 5. The dark and light shadows indicate the 50% and 95% confidence intervals derived from bootstrap analyses, respectively.

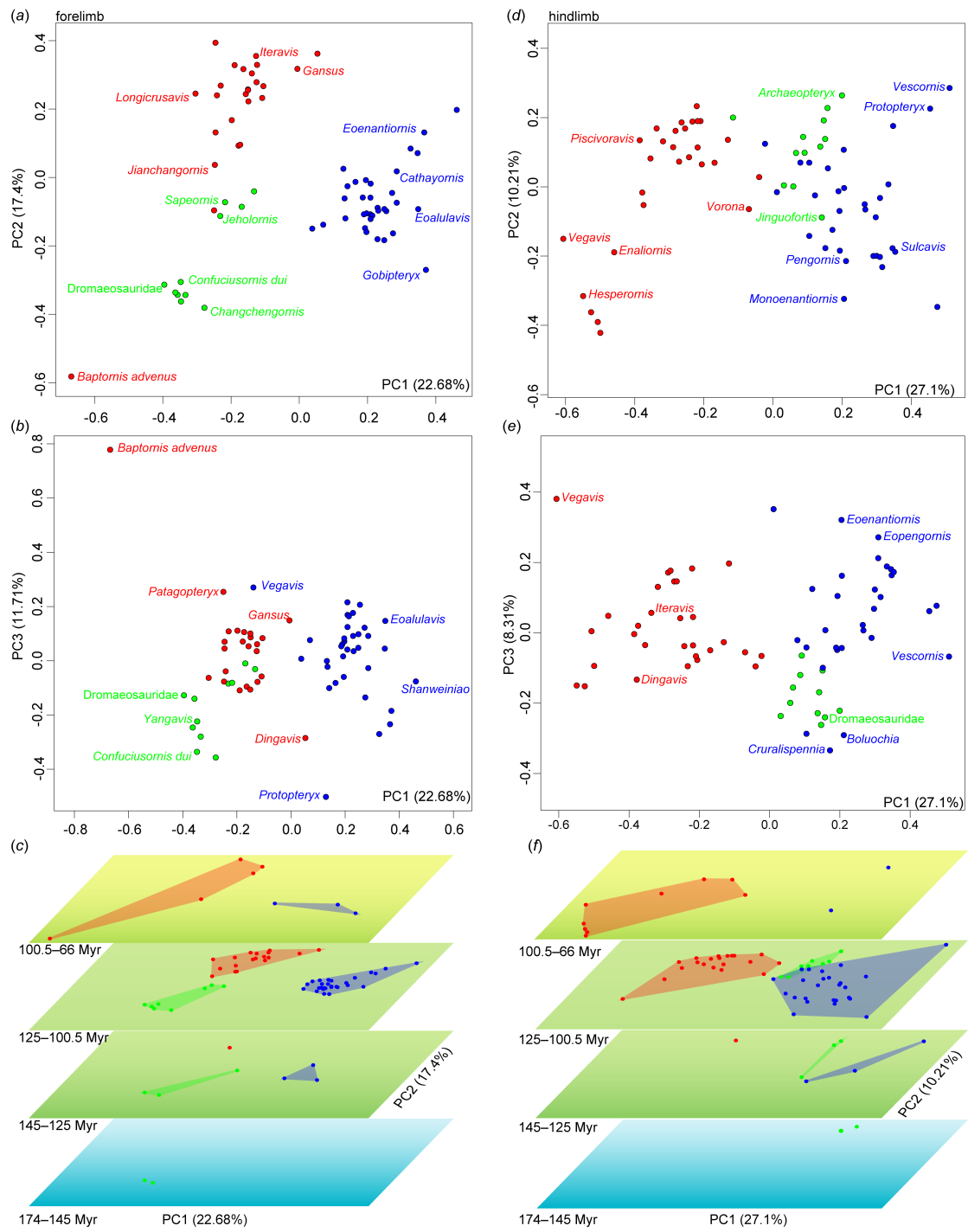


Figure S35. Discrete character morphospace of the fore- and hindlimb of Mesozoic birds. The phylogenetic backbone is the “mbl”-scaled phylogeny, and MORD was used as the distance metrics. Pairwise binary plot of pcoas 1–3 and stacked from the Late Jurassic to Cretaceous of the forelimb (a–c), and hindlimb (d–f), respectively.

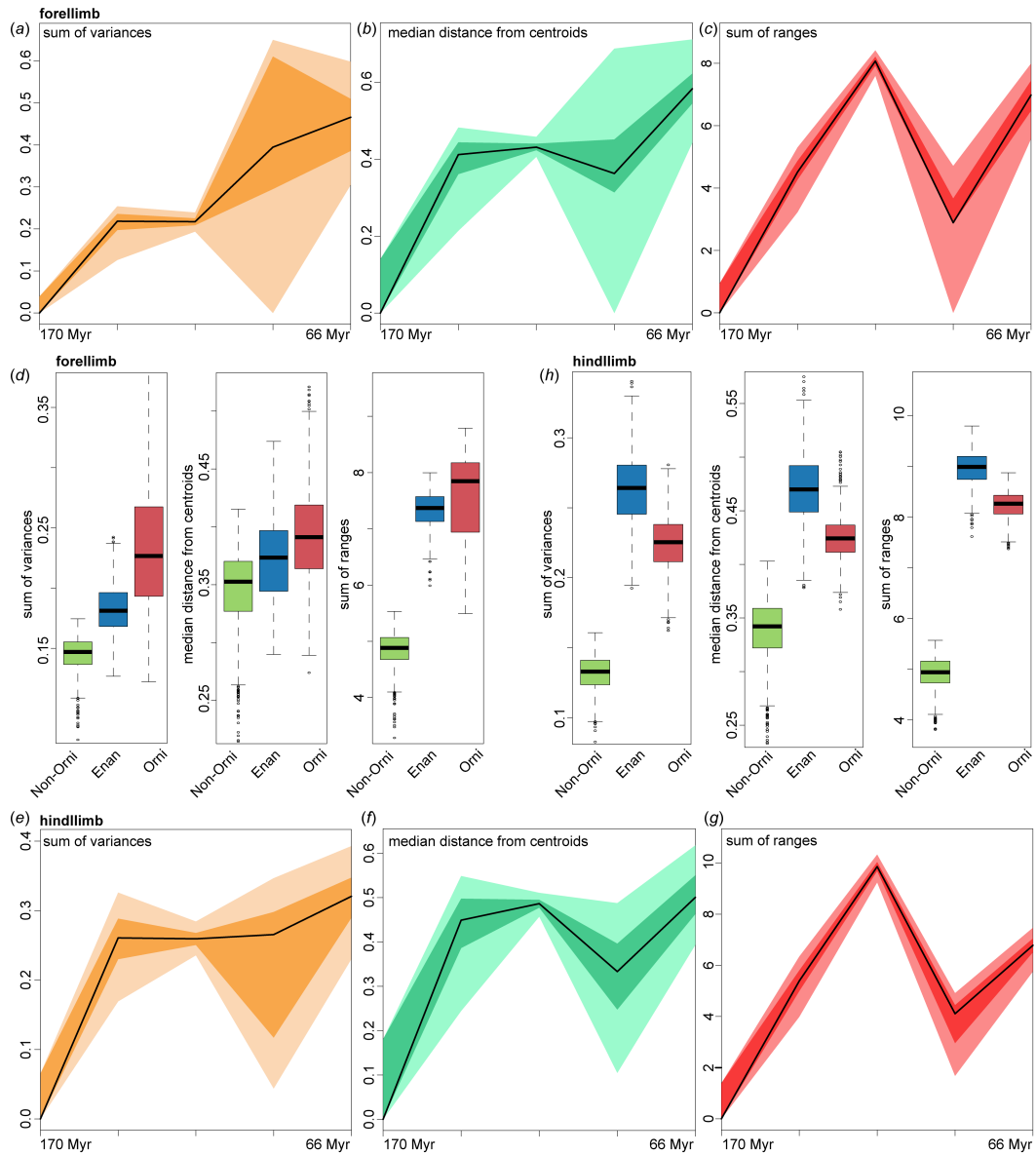


Figure S36. Morphological disparity of the fore- and hindlimb of Mesozoic birds.

The phylogenetic backbone is derived from “mbl”-scaled strict consensus tree, and MORD was used as the distance metrics. (a–c) Disparity curves of the forelimb, and (e–f) hindlimb morphology of Mesozoic birds as a whole across five time bins as defined in figure 5; (d) box plots showing disparity metrics among groups demonstrated in forelimb, and hindlimb (h), respectively. The dark and light shadows indicate the 50% and 95% confidence intervals derived from bootstrap analyses, respectively.

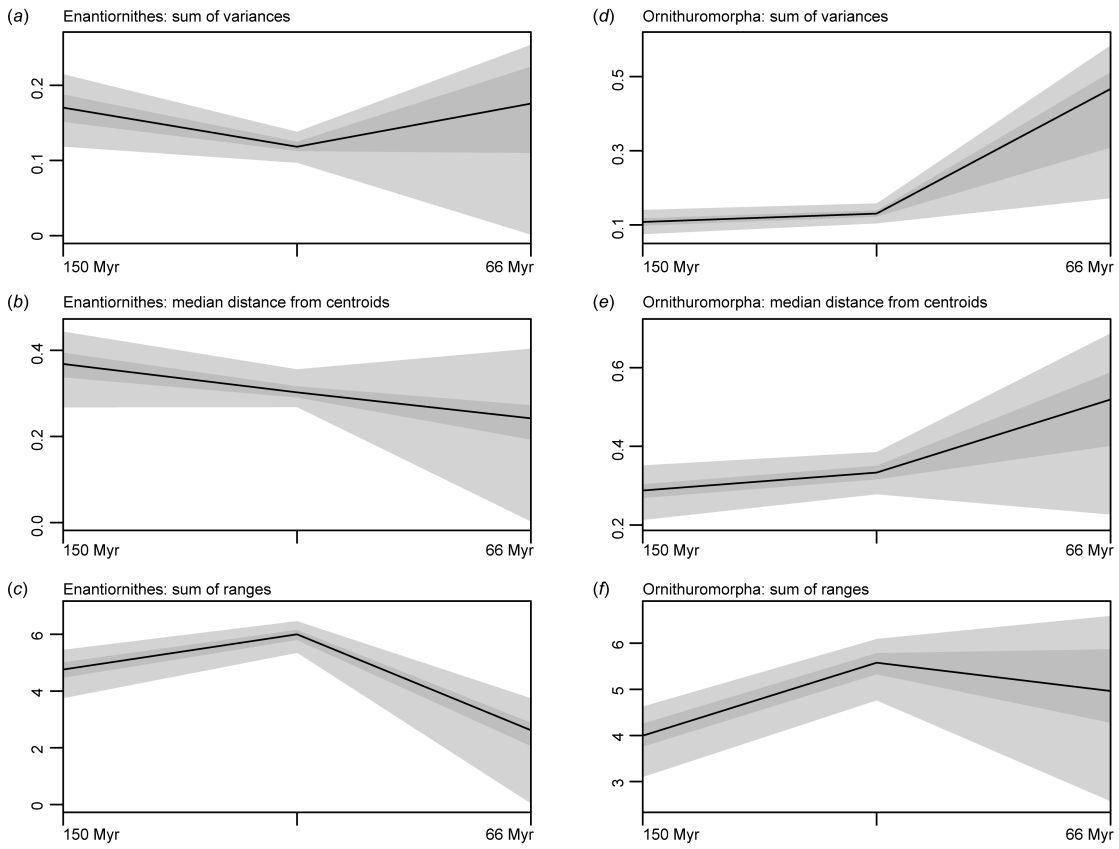


Figure 37. Comparison of forelimb morphological disparity between Enantiornithes and Ornithuromorpha. The phylogenetic backbone is the “mbl”-scaled phylogeny, and MORD was used as the distance metrics. Three disparity metrics are shown: sum of variance (a,d), median distance from centroid (b,e), and sum of ranges (c,f). Disparity curves are binned into subequal-length time bins as defined in figure 5. The dark and light shadows indicate the 50% and 95% confidence intervals derived from bootstrap analyses, respectively.

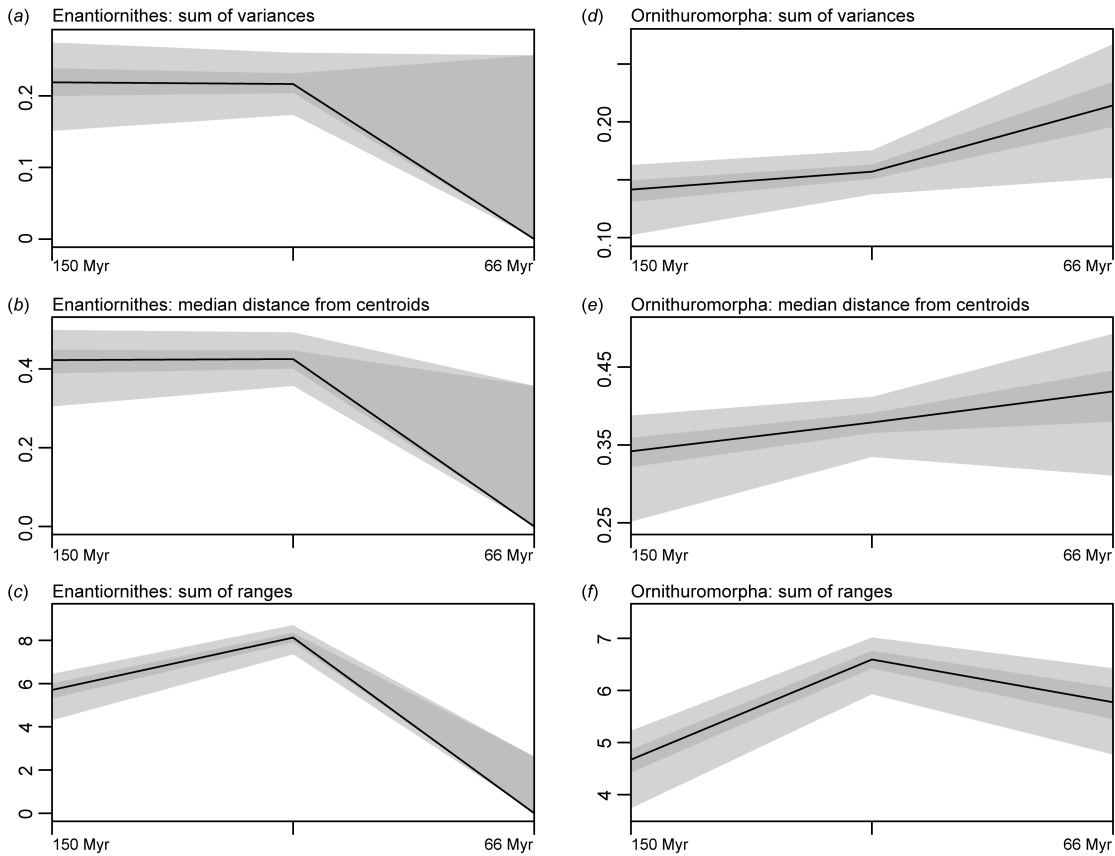


Figure 38. Comparison of hindlimb morphological disparity between Enantiornithes and Ornithuromorpha. The phylogenetic backbone is the “mbl”-scaled phylogeny, and MORD was used as the distance metrics. Three disparity metrics are shown: sum of variance (a,d), median distance from centroid (b,e), and sum of ranges (c,f). Disparity curves are binned into subequal-length time bins as defined in figure 5. The dark and light shadows indicate the 50% and 95% confidence intervals derived from bootstrap analyses, respectively.

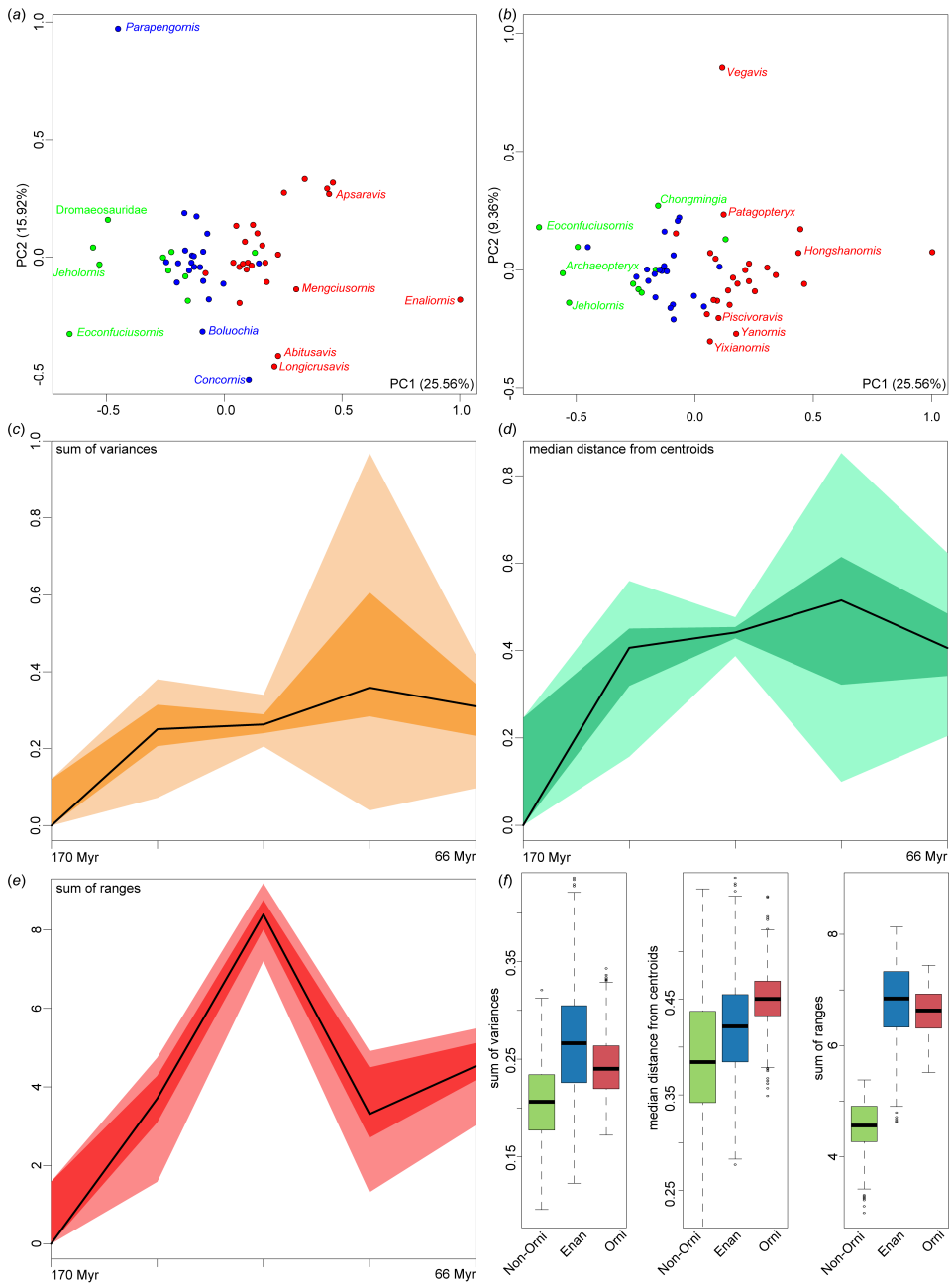


Figure S39. Morphological disparity of the pelvis of Mesozoic birds. The phylogenetic backbone is derived from “mbl”-scaled strict consensus tree, and MORD was used as the distance metrics. (a,b) Pairwise binary plot of pcoa 1–3; (c–e) disparity curves of Mesozoic birds as a whole across five time bins as defined in figure 5; (f) box plots showing disparity metrics among groups. The dark and light shadows indicate the 50% and 95% confidence intervals derived from bootstrap analyses, respectively.

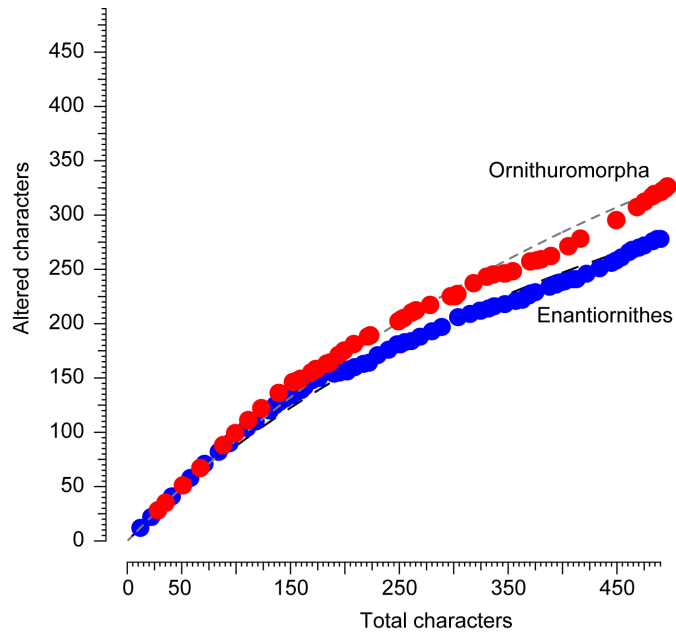


Figure S40. Exhaustion of the totable number of character alterations against numbers of characters. The red circles denote the Ornithuromorpha, and the blue ones denote the Enantiornithes.

1. Zhang C, Wang M. 2019 Bayesian tip dating reveals heterogeneous morphological clocks in mesozoic birds. *Royal Society Open Science* **6**, 182062. (doi:10.1098/rsos.182062)
2. Lewis PO. 2001 A likelihood approach to estimating phylogeny from discrete morphological character data. *Systematic Biology* **50**, 913-925. (doi:10.1080/106351501753462876)
3. Yang Z. 1994 Maximum likelihood phylogenetic estimation from DNA sequences with variable rates over sites: Approximate methods. *Journal of Molecular Evolution* **39**, 306-314. (doi:10.1007/BF00160154)
4. Stadler T. 2010 Sampling-through-time in birth-death trees. *Journal of Theoretical Biology* **267**, 396-404. (doi:<https://doi.org/10.1016/j.jtbi.2010.09.010>)
5. Drummond AJ, Ho SY, Phillips MJ, Rambaut A. 2006 Relaxed phylogenetics and dating with confidence. *PLoS biology* **4**.
6. Ronquist F, Teslenko M, van der Mark P, Ayres DL, Darling A, Höhna S, Larget B, Liu L, Suchard MA, Huelsenbeck JP. 2012 Mrbayes 3.2: Efficient bayesian phylogenetic inference and model choice across a large model space. *Systematic Biology* **61**, 539-542. (doi:10.1093/sysbio/sys029)
7. Brougham T, Campione NE. 2020 Body size correlates with discrete-character morphological proxies. *Paleobiology* **46**, 304-319.
8. Wagner PJ. 2000 Exhaustion of morphologic character states among fossil taxa. *Evolution* **54**, 365-386. (doi:10.1111/j.0014-3820.2000.tb00040.x)
9. Bapst DW. 2012 Paleotree: An r package for paleontological and phylogenetic analyses of evolution. *Methods in Ecology and Evolution* **3**, 803-807. (doi:10.1111/j.2041-210X.2012.00223.x)